Supplementary Information

# From Local to Global or Semilocal Aromaticity: Singlet–Triplet Switching in Porphyrin Tapes

Sergio Moles Quintero,[a] Luis Álvarez-Thon,[b] William Tiznado[*,c] Luis Leyva-Parra,[*,c] and Mercedes Alonso[*,a]

[a]*Department of General Chemistry (ALGC), Vrije Universiteit Brussel (VUB), Pleinlaan 2, 1050 Brussels; Belgium.*

[b]*Centro de Investigación en Ingeniería de Materiales (CIIMAT), Facultad de Ingeniería y Arquitectura, Universidad Central de Chile (UCEN), Santa Isabel 1186, 8370146, Santiago, Chile.*

[c]*Centro de Investigación para el Diseño de Materiales (CEDEM), Facultad de Ciencias Exactas, Departamento de Ciencias Químicas, Universidad Andrés Bello, Avenida República 275, Santiago 837014, Chile*

*Correspondence: luis.leyva@unab.cl (LL-P); mercedes.alonso.giner@vub.be (MA); wtiznado@unab.cl (WT).*

Table of contents

## Computational Details

The molecular structures of the porphyrin tapes (PT) were optimized using the Gaussian 16 program[1] at the ωB97X-D[2]/def2-TZVP[3] level of theory. $T_1$-state geometries were optimized using the unrestricted formalism, while the restricted formalism was employed for closed-shell singlet states. The calculations of harmonic vibrational frequencies, employing the aforementioned level of theory, confirmed that all optimized structures correspond to true minima on the potential energy surface. The use of a range-separated hybrid functional is motivated by previous studies showing that long-range Hartree–Fock exchange is essential for a realistic description of electron delocalization in extended π-conjugated and macrocyclic systems, where conventional hybrid functionals may overestimate cyclic delocalization.[4] Singlet–triplet energy gaps ($\Delta E_{ST}$) were obtained from single-point DLPNO-CCSD(T1)[5-7]/def2-TZVP calculations on geometries optimized at the ωB97X-D/def2-TZVP level. All DLPNO calculations were performed with the ORCA 6.0.1 package.[8] The single-reference character of the wavefunction was assessed through the $T_1$ diagnostic[9] computed from the DLPNO-CCSD(T1) results, yielding values below 0.02 for all low-energy isomers. The Cartesian coordinates of the optimized structures can be found in the end of this SI.

Magnetically induced current density (MICD) calculations were carried out using the SYSMOIC program package.[10] An external magnetic field was applied along the z-axis, perpendicular to the molecular plane of PT systems, and the CTOCD-DZ method was used to ensure origin-independent results.[11] Molecular orbitals and magnetic properties were first computed in Gaussian 16 using the CSGT (Continuous Set of Gauge Transformations) formalism to generate the necessary unperturbed and perturbed wavefunctions.[12] These wavefunctions were subsequently employed in SYSMOIC to compute current density vector fields. The diatropic (clockwise) ring currents are indicative of aromatic stabilization, while the paratropic (counterclockwise) currents suggest antiaromatic character. The ring current strengths (RCS, in $nA.T^{-1}$) were evaluated according to the SYSMOIC definition of net bond current strengths. The integration of the π-component of the magnetically induced current density through planes bisecting selected atom–atom pairs (bond-crossing sections) was performed, with the integration domain defined by current-density contours close to zero. This approach affords a local, topology-resolving measure of current flow, thereby facilitating the identification of current continuity and bottlenecks at junctions within extended π-conjugated systems. Isochemical Shielding Surface (ICSS) [13, 14] calculations were performed at the ωB97X-D/def2-TZVP level of theory to complement the magnetic response analysis. The calculations were carried out using the Multiwfn program package.[15] ICSS maps offer a spatial representation of magnetic shielding and deshielding regions, thereby serving as a qualitative descriptor of aromatic and antiaromatic behavior. Isosurface plots were used to visualize the magnetic response of the porphyrin tapes in both $S_0$ and $T_1$ states.

To assess the extent of π-electron delocalization in the investigated systems, Electron Density of Delocalized Bonds (EDDB)[16, 17] calculations were performed at the ωB97X-D/def2-TZVP level of theory. It has been demonstrated in previous studies that EDDB results demonstrate minimal sensitivity to basis set size. Specifically for this work, the $EDDB_H$ and $EDDB_P$ functions have been used, the latter of which has been shown in the literature to be a descriptor of aromaticity for local rings. To complement the EDDB analysis, aromaticity was further quantified using a combination of geometric- and electron-delocalization-based descriptors. Structural aromaticity was evaluated through the harmonic oscillator model of aromaticity (HOMA),[18] defined as

$$HOMA(\mathcal{A}) = 1 - \frac{\alpha}{n}\sum_{i=1}^{n}\left(R_{opt} - R_i\right)^2$$

where α is an empirical constant associated with the bond type, $n$ is the number of bonds along the selected conjugation pathway $\mathcal{A}$, $R_i$ are the individual bond lengths, and $R_{opt}$ corresponds to the optimal reference bond length for a fully aromatic system. HOMA values close to unity are indicative of aromatic character, whereas values near zero are typical of nonaromatic systems; negative values are commonly associated with antiaromatic monocyclic rings.

Electronic aromaticity descriptors were evaluated within the framework of the Quantum Theory of Atoms in Molecules (QTAIM). In this context, the para-delocalization index (PDI) was employed as a local aromaticity criterion for six-membered rings. Within QTAIM, the delocalization index (DI) between atoms $A$ and $B$, $\delta(A,B)$for a closed-shell wavefunction is given by

$$\delta(A,B) = 4\sum_{i,j} S_{ij}(A)S_{ij}(B)$$

where the summations run over occupied molecular orbitals and $S_{ij}(A)$ and $S_{ij}(B)$ are elements of the atomic overlap matrices of atoms $A$ and $B$, respectively.[19]

To account for multicenter electron delocalization effects, the multicenter index (MCI) was also computed.[20] MCI is a generalization of the Iring index that explicitly considers all possible permutations of the atomic centers forming the ring and is defined as

$$MCI(\mathcal{A}) = \frac{2^{n-1}}{n}\sum_{\mathcal{P}(\mathcal{A})}\sum_{i_1,i_2,\ldots,i_n}^{occ} S_{i_1,i_2,}(A_1)S_{i_2,i_3,}(A_2),\ldots S_{i_n,i_{n+1},}(A_n)$$

where $\mathcal{P}(\mathcal{A})$ denotes the $n!$ permutations of the atomic centers within ring $A$. MCI values close to zero are characteristic of nonaromatic systems, whereas larger values indicate aromatic behavior. For larger rings, where the computational cost and numerical instabilities associated with MCI become significant, the AV1245 and $AV_{min}$ indices were employed. AV1245 corresponds to the average of four-center MCI values involving atoms at positions 1, 2, 4, and 5 along consecutive five-atom fragments of the ring,[21,22] whereas $AV_{min}$ is defined as the minimum absolute value among these four-center contributions.[22] Both indices yield large values for aromatic systems and small values for nonaromatic or antiaromatic species.

In addition, the aromatic fluctuation index (FLU) was evaluated as a complementary electronic descriptor that quantifies the degree of uniformity of electron delocalization along the ring.[23] FLU is defined as

$$FLU(\mathcal{A}) = \frac{1}{n}\sum_{i=1}^{n}\left(\frac{\delta(A_i)}{\delta(A_{i-1})}\right)^{\alpha}\left(\frac{\delta(A_i,A_{i-1}) - \delta_{ref}(A_i,A_{i-1})}{\delta_{ref}(A_i,A_{i-1})}\right)^2$$

where $\delta(A_i,A_{i-1})$ is the delocalization index between two adjacent atoms in the ring, $\delta(A_i)$ and $\delta(A_{i-1})$ are the atomic delocalization indices, $\delta_{ref}(A_i,A_{i-1})$ is a reference value corresponding to an ideal aromatic system, and $\alpha$ is an empirical exponent introduced to account for bond polarity effects. Low FLU values indicate a uniform distribution of electron delocalization and are therefore characteristic of aromatic systems, whereas larger values reflect increased electronic fluctuation and reduced aromatic character.

The electronic aromaticity indices, FLU, AV1245 and $AV_{min}$ and the structural HOMA indice were computed within the Quantum Theory of Atoms in Molecules (QTAIM)[24,26] framework, using the atomic partitioning scheme implemented in the AIMAll software.[26-29] The resulting atomic overlap matrices, along with the

wavefunction files, were subsequently used as input for the ESI-3D code.[30] The numerical integration error for all atomic basins in the QTAIM analysis was kept below 0.04 electrons.

## Discussion of AV1245 distribution values for $PT_2$, $PT_3$ and $PT_4$

The aromaticity of $PT_2$ was further examined using the AV1245 index, which quantifies average electron delocalization between bonds 1–2 and 4–5 in rings with more than six members. When evaluated over the full conjugation pathway, the $S_0$ state exhibits a higher average value (1.39) than $T_1$ (0.12), indicating stronger delocalization in the ground state. However, because this is an averaged descriptor, its spatial distribution provides more meaningful insights. As shown in Figure 4 in manuscript, the $S_0$ state generally displays higher AV1245 values along the periphery, except for two regions—highlighted in grey—where $T_1$ shows enhanced delocalization. This pattern agrees with the $EDDB_H$ and RCS analyses, confirming the emergence of global aromaticity in $T_1$. Within the central naphthalene segment, AV1245 values are higher for $S_0$ than for $T_1$, in line with the π-current density data, while the outer porphyrin retains the same trend, consistent with $ICSS_{zz}$ isosurfaces.

For $PT_3$, Figure S5 show the AV1245 profile of the outer porphyrin in $S_0$ closely resembles that of $PT_2$, suggesting the persistence of local aromatic character. Upon excitation, the $T_1$ values become comparable to those of $S_0$, indicating a shift from global to more localized delocalization. In the inner pathway, two regions exhibit increased AV1245 values in $T_1$, consistent with the RCS data. The magnitude of these variations depends on the criterion used—RCS or AV1245—reflecting the conceptual differences between magnetic and electronic indices.

The AV1245 distribution in $PT_4$ follows the same overall trend (Figure S8). Along the outer pathway, the $S_0$ and $T_1$ states display nearly indistinguishable values, matching the uniform RCS response in this region. In contrast, the central segment, comprising two inner porphyrins, reveals alternating domains: the $S_0$ state shows higher AV1245 values in the lateral sections, whereas the $T_1$ state presents enhanced delocalization in the remaining four-membered sequences. These findings are consistent with the current density isosurfaces and confirm that, as the number of fused units increases, the system evolves from a global to a semilocal aromatic regime in the triplet state.

## $PT_2$

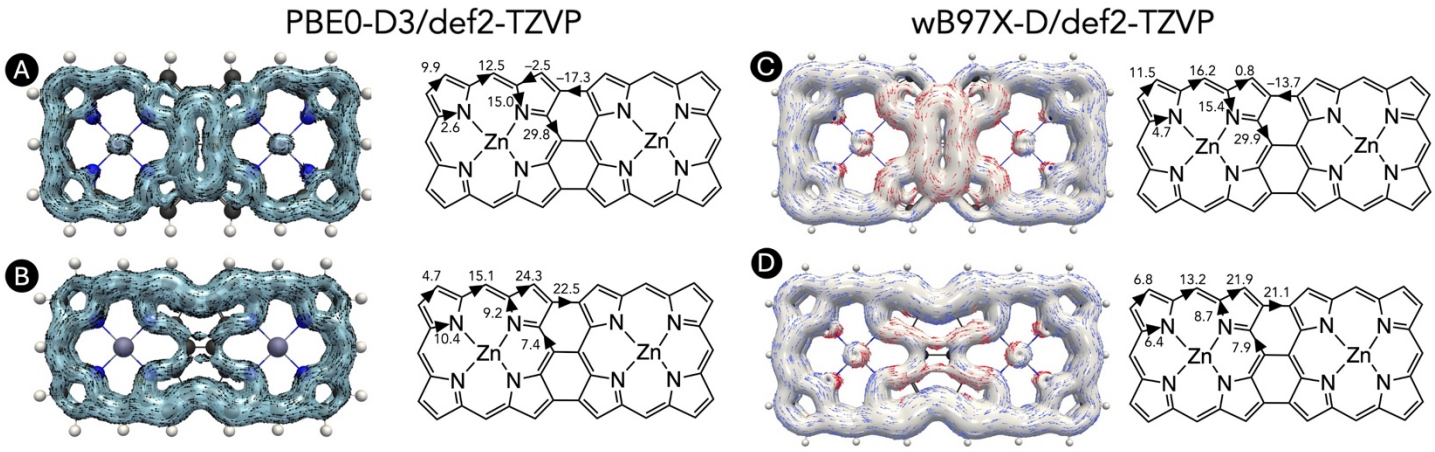


**Figure S1**. π-only current density isosurfaces (isovalue = 0.02) and flow intensity values (in nA $T^{-1}$) for $PT_2$ in the $S_0$ (A,C) and $T_1$ (B,D) states. computed at PBE0-D3/def2-TZVP (right) and ωB97X-D/def2-TZVP level (left).

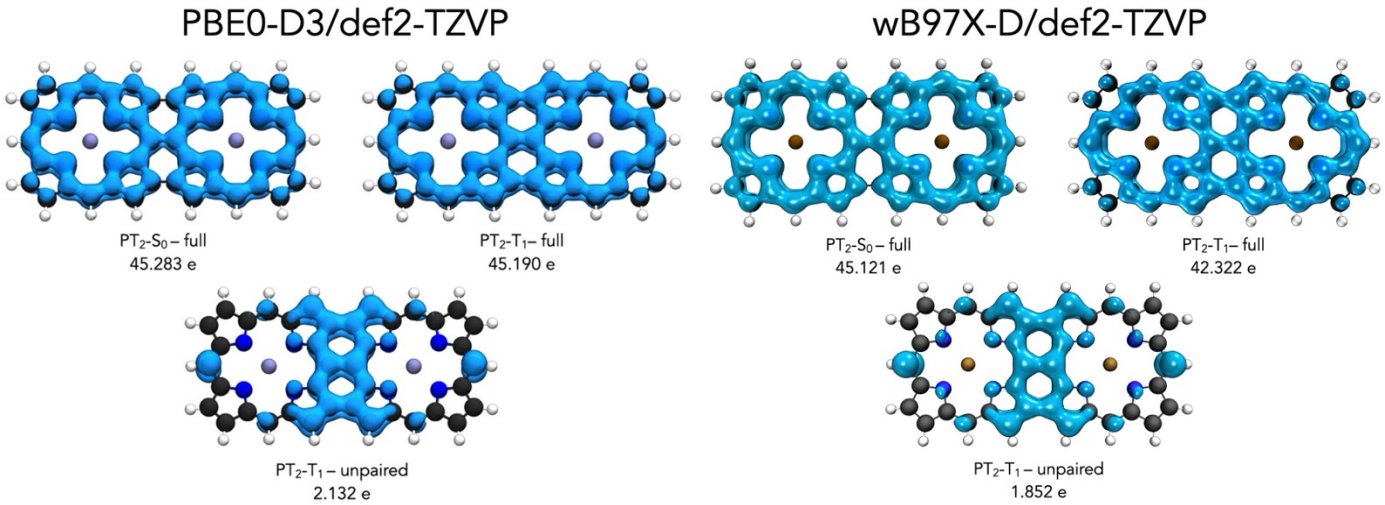


**Figure S2**. $EDDB_H$ isosurfaces (±0.02) for $PT_2$. The $EDDB_H$-unpaired surface (±0.002) shows cyclic delocalization in the central region. The total number of delocalized electrons is shown. computed at PBE0-D3/def2-TZVP (right) and ωB97X-D/def2-TZVP level (left).

**$PT_3$**

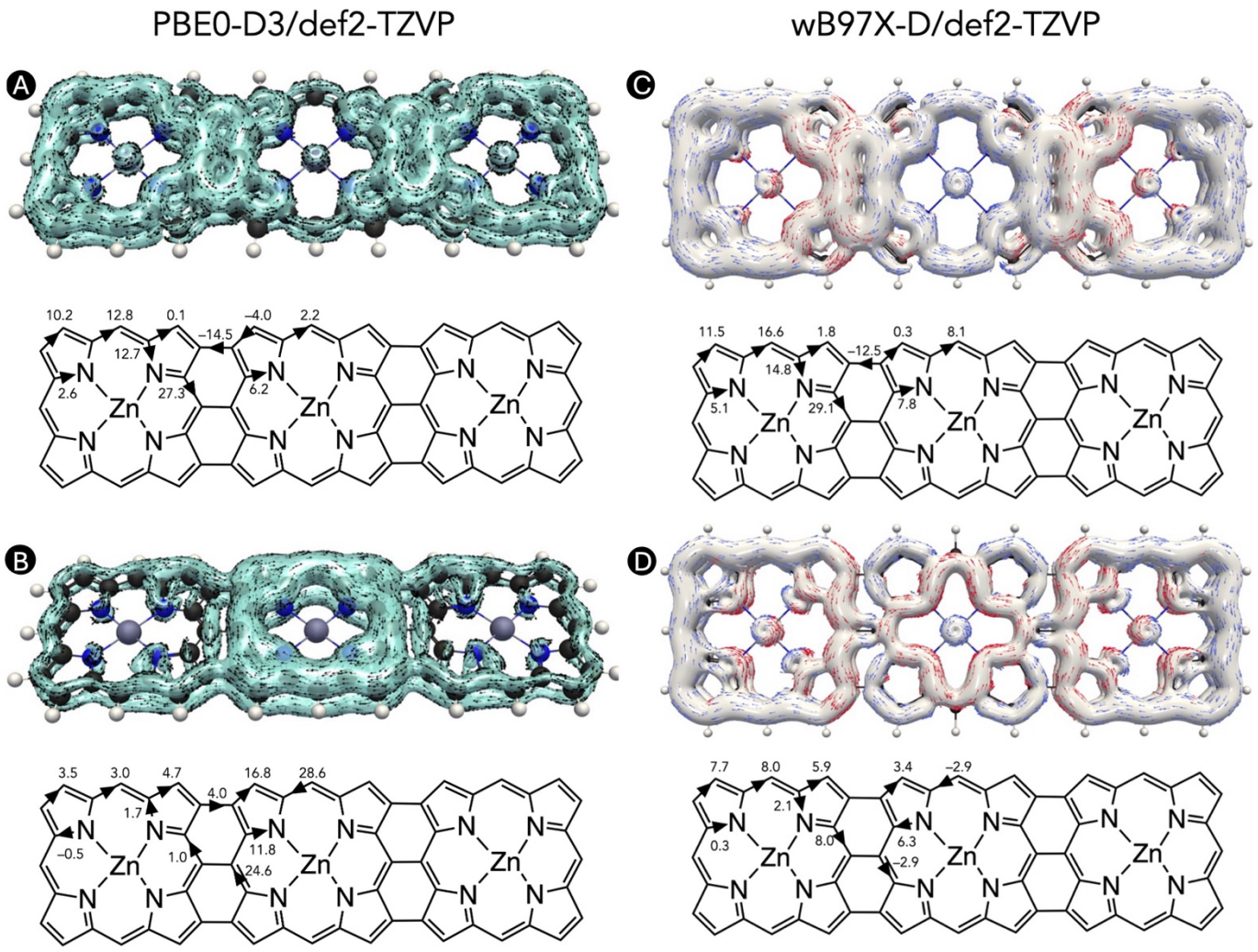


**Figure S3**. π-only current density isosurfaces (isovalue = 0.02) and flow intensity values (in nA $T^{-1}$) for $PT_3$ in the $S_0$ (A,C) and $T_1$ (B,D) states. computed at PBE0-D3/def2-TZVP (right) and ωB97X-D/def2-TZVP level (left).

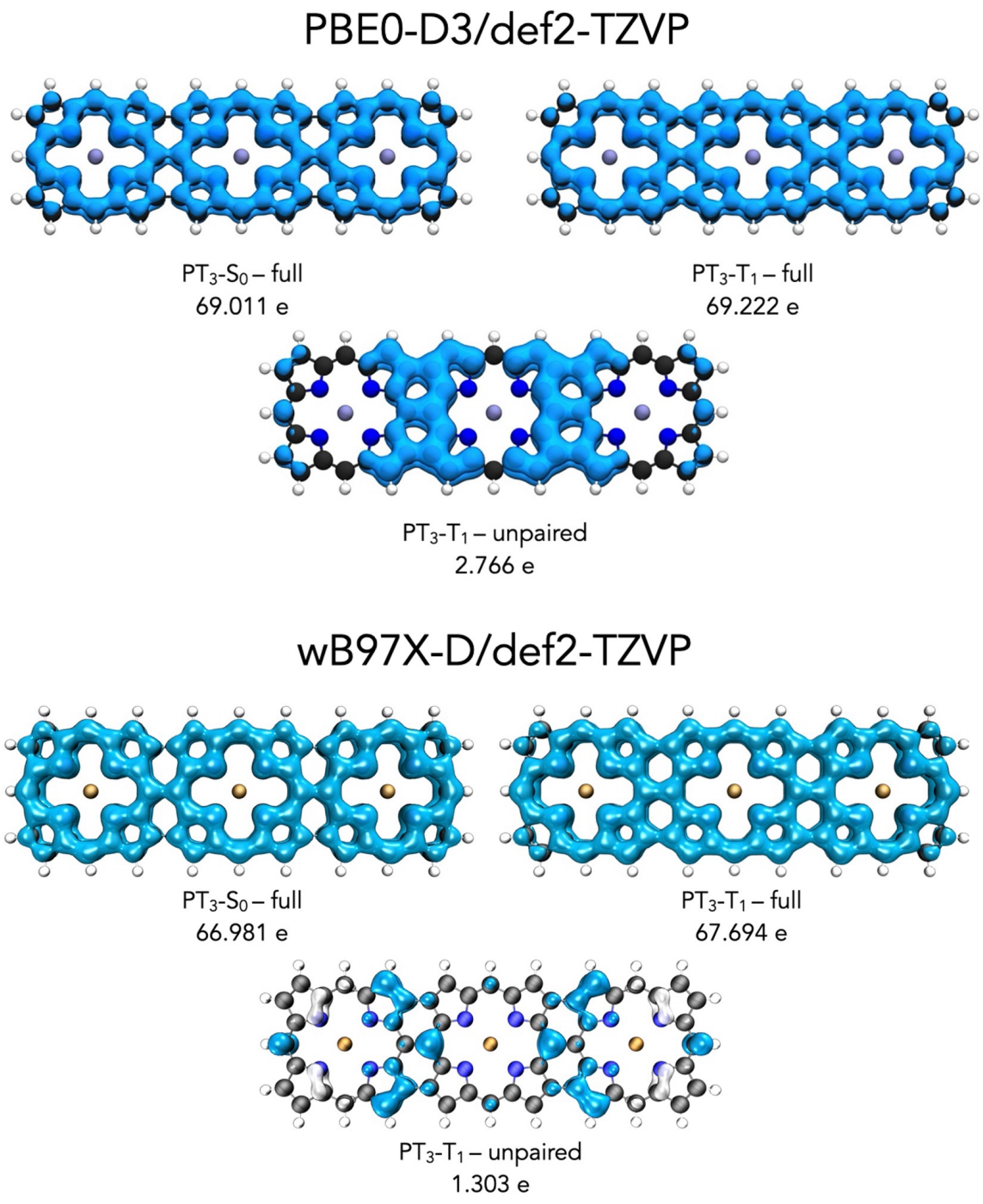


**Figure S4**. $EDDB_H$ isosurfaces (±0.02) for $PT_3$. The $EDDB_H$-unpaired surface (±0.002) shows cyclic delocalization in the central region. The total number of delocalized electrons is shown. computed at PBE0-D3/def2-TZVP (top) and ωB97X-D/def2-TZVP level (bottom).

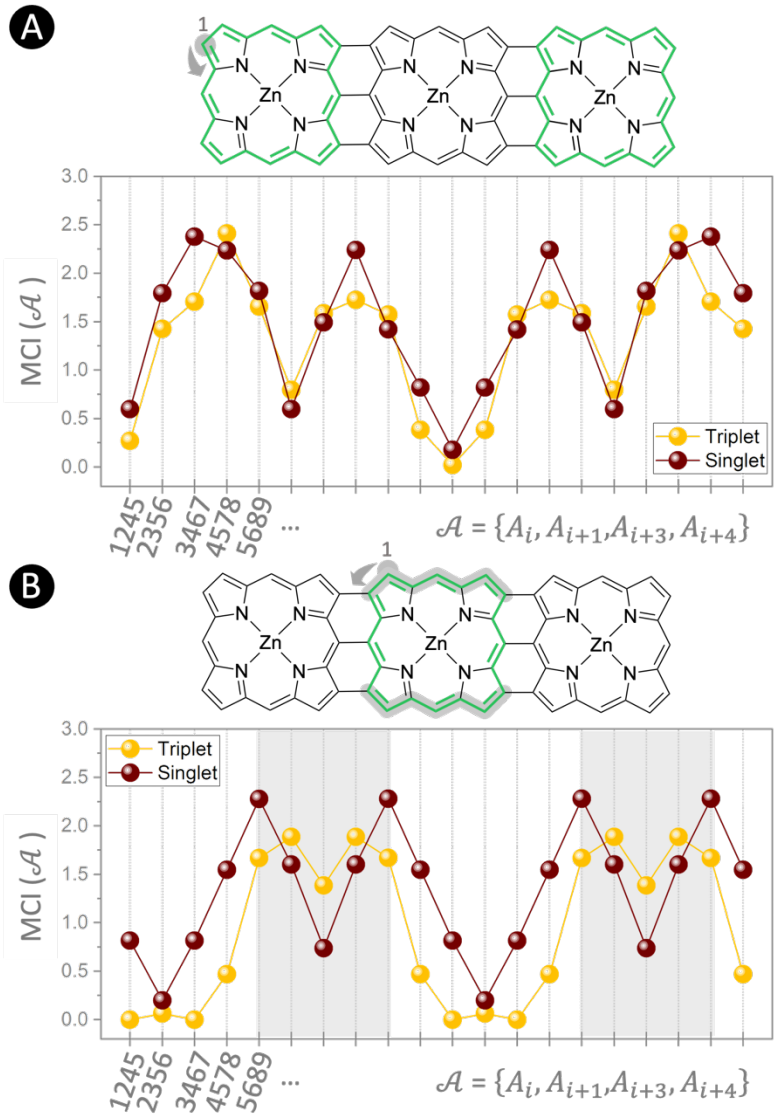


**Figure S5**. AV1245 index distribution along the outer (A) and inner (B) porphyrin pathways (in green) of $PT_3$ for the $S_0$ and $T_1$ states. The grey-highlighted atom marks the first atom of the reference fragment used in the AV1245 calculation, and the grey arrow indicates the direction of the x-axis. Grey-shaded regions correspond to AV1245 values derived from the carbon atom sequences highlighted in grey on the molecular structure.

## $PT_4$

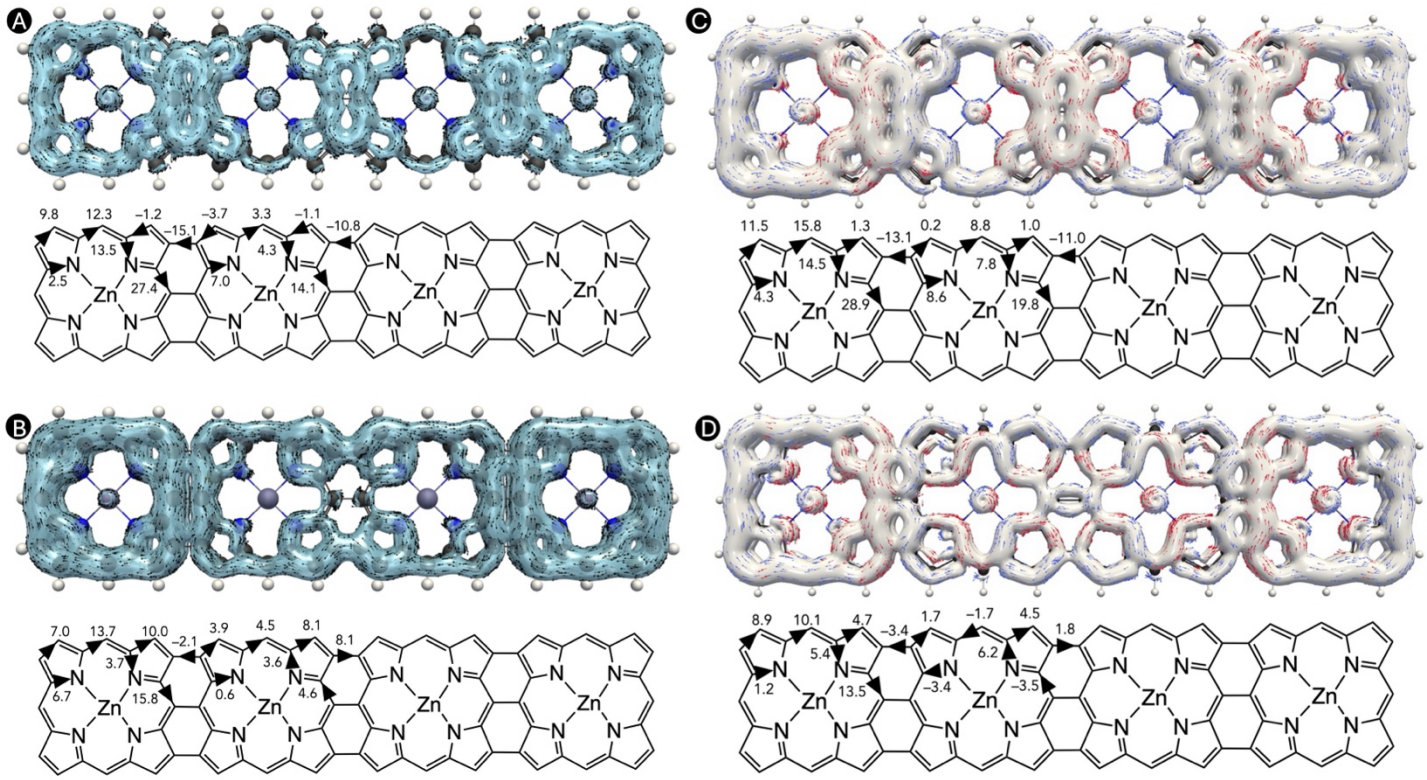


**Figure S6**. π-only current density isosurfaces (isovalue = 0.02) and flow intensity values (in nA $T^{-1}$) for $PT_4$ in the $S_0$ (A,C) and $T_1$ (B,D) states. computed at PBE0-D3/def2-TZVP (right) and ωB97X-D/def2-TZVP level (left).

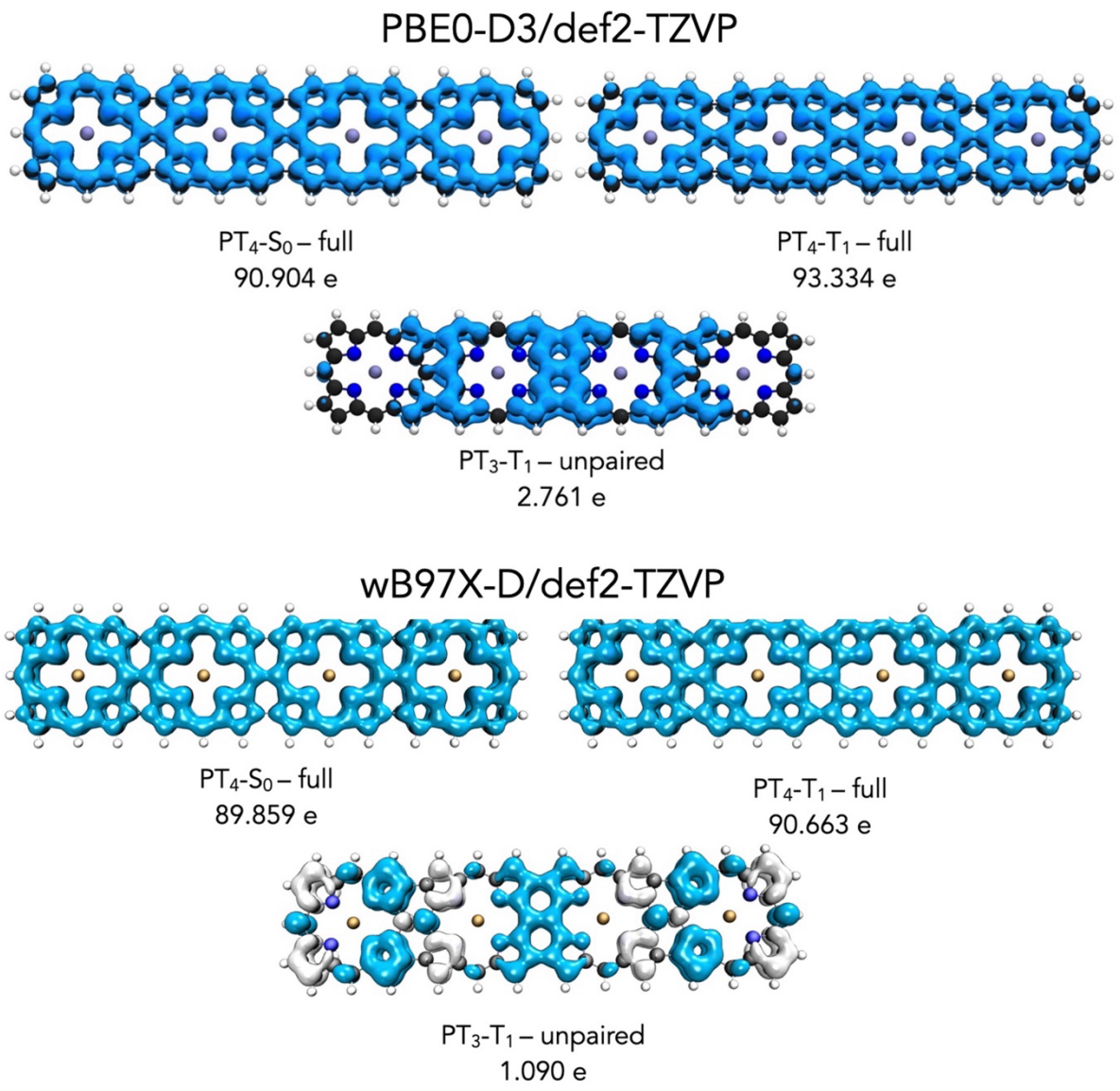


**Figure S7**. $EDDB_H$ isosurfaces (±0.02) for $PT_4$. The $EDDB_H$-unpaired surface (±0.002) shows cyclic delocalization in the central region. The total number of delocalized electrons is shown. computed at PBE0-D3/def2-TZVP (top) and ωB97X-D/def2-TZVP level (bottom).

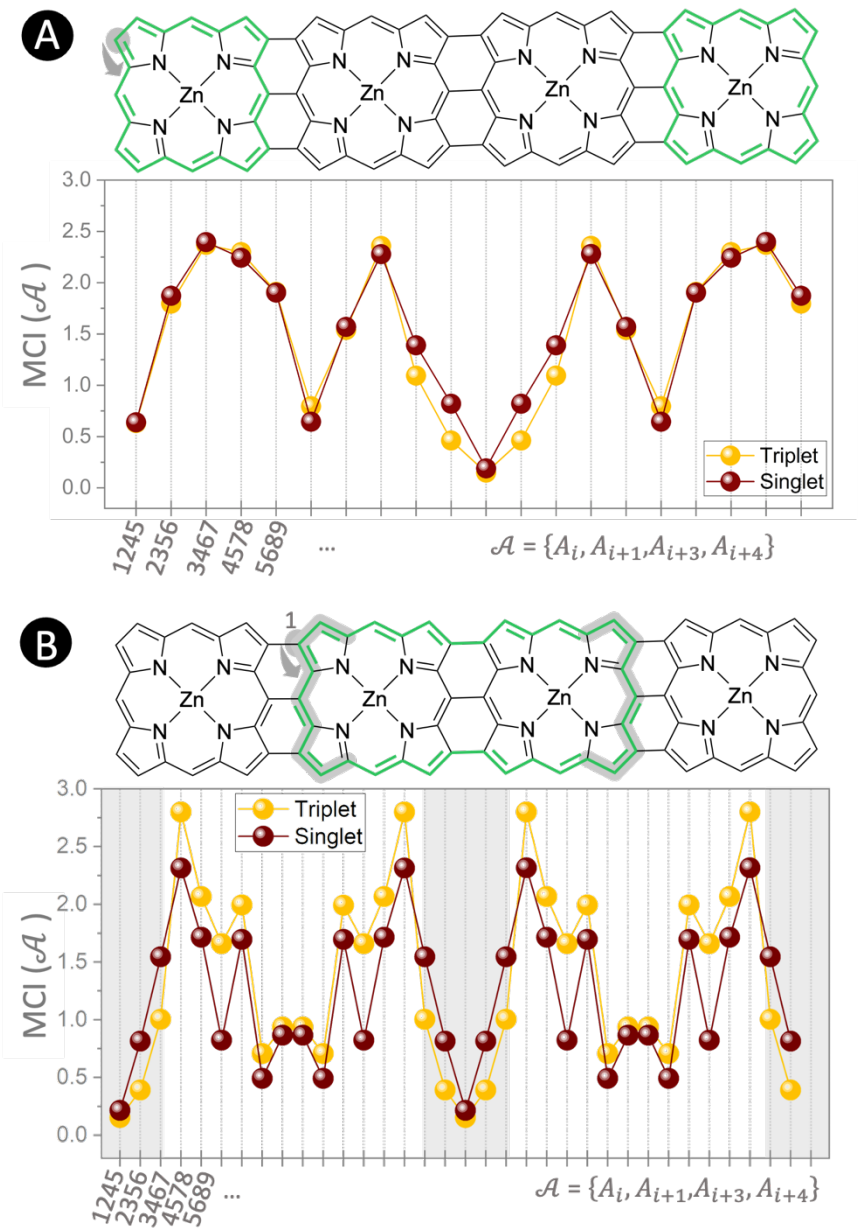


**Figure S8**. AV1245 index distribution along the outer (A) and inner (B) porphyrins pathways (in green) of PT3 for the $S_0$ and $T_1$ states. The grey-highlighted atom marks the first atom of the reference fragment used in the AV1245 calculation, and the grey arrow indicates the direction of the x-axis. Grey-shaded regions correspond to AV1245 values derived from the carbon atom sequences highlighted in grey on the molecular structure.

## Additional aromaticity indices

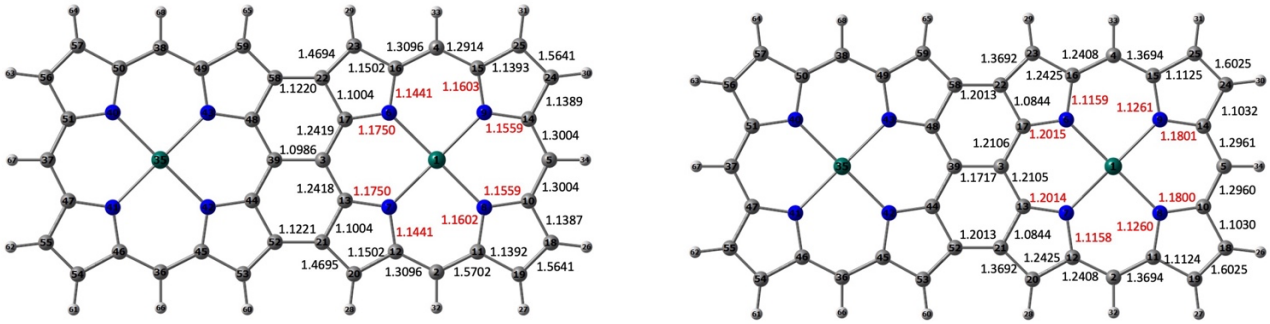


**Figure S9**. Delocalization indices for $PT_2$ in $S_0$ (top) and $T_1$ (bottom), computed at PBE0-D3/def2-TZVP level of theory. Inner bonds are highlighted in red.

**Table S1**. Aromaticity indices for the selected circuits $PT_2$ in $S_0$.

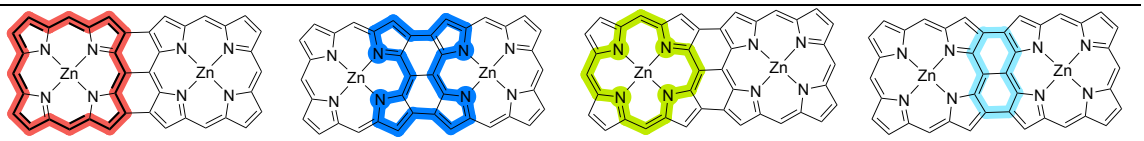

| | Ring circuit 1 | | Ring circuit 2 | | Ring circuit 3 | | Ring circuit 4 | |
|---|---|---|---|---|---|---|---|---|
| | PBE0-D3 | ωB97X-D | PBE0-D3 | ωB97X-D | PBE0-D3 | ωB97X-D | PBE0-D3 | ωB97X-D |
| FLU | 0.0201 | 0.0208 | 0.0132 | 0.0144 | 0.0046 | 0.0040 | 0.0336 | 0.0341 |
| HOMA | 0.7130 | 0.6862 | 0.7980 | 0.7566 | 0.9580 | 0.9620 | 0.6020 | 0.5710 |
| AV1245 | 1.5340 | 1.5600 | –0.6490 | -0.6820 | 0.9750 | 0.9780 | 0.2780 | 0.2520 |
| $AV_{min}$ | 0.1850 | 0.2100 | –7.8460 | -7.8350 | 0.4660 | 0.3690 | 0.1330 | 0.1020 |
| $EDDB_P$[a] | 5.0797 | | 5.2913 | | 8.5349 | | 1.5550 | |

[a]Computed at ωB97X-D/def2-TZVP

**Table S2**. Aromaticity indices for the selected circuits for $PT_2$ in $T_1$.

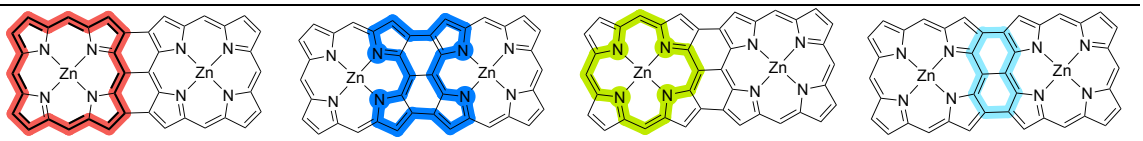

| | Ring circuit 1 | | Ring circuit 2 | | Ring circuit 3 | | Ring circuit 4 | |
|---|---|---|---|---|---|---|---|---|
| | PBE0-D3 | ωB97X-D | PBE0-D3 | ωB97X-D | PBE0-D3 | ωB97X-D | PBE0-D3 | ωB97X-D |
| FLU | 0.0220 | 0.0240 | 0.0092 | 0.0084 | 0.0065 | 0.0096 | 0.0346 | 0.0328 |
| HOMA | 0.6690 | 0.6028 | 0.9050 | 0.9146 | 0.9240 | 0.9016 | 0.5760 | 0.6181 |
| AV1245 | 1.0650 | 0.9520 | –0.4340 | -0.4830 | 0.8640 | 0.8750 | 0.1590 | 0.1860 |
| $AV_{min}$ | 0.0420 | 0.022 | –7.4280 | -7.5430 | –0.0250 | -0.0810 | –0.1030 | -0.175 |
| $EDDB_P$[a] | 2.6052 | | 9.6366 | | 5.1047 | | 2.3316 | |

[a]Computed at ωB97X-D/def2-TZVP

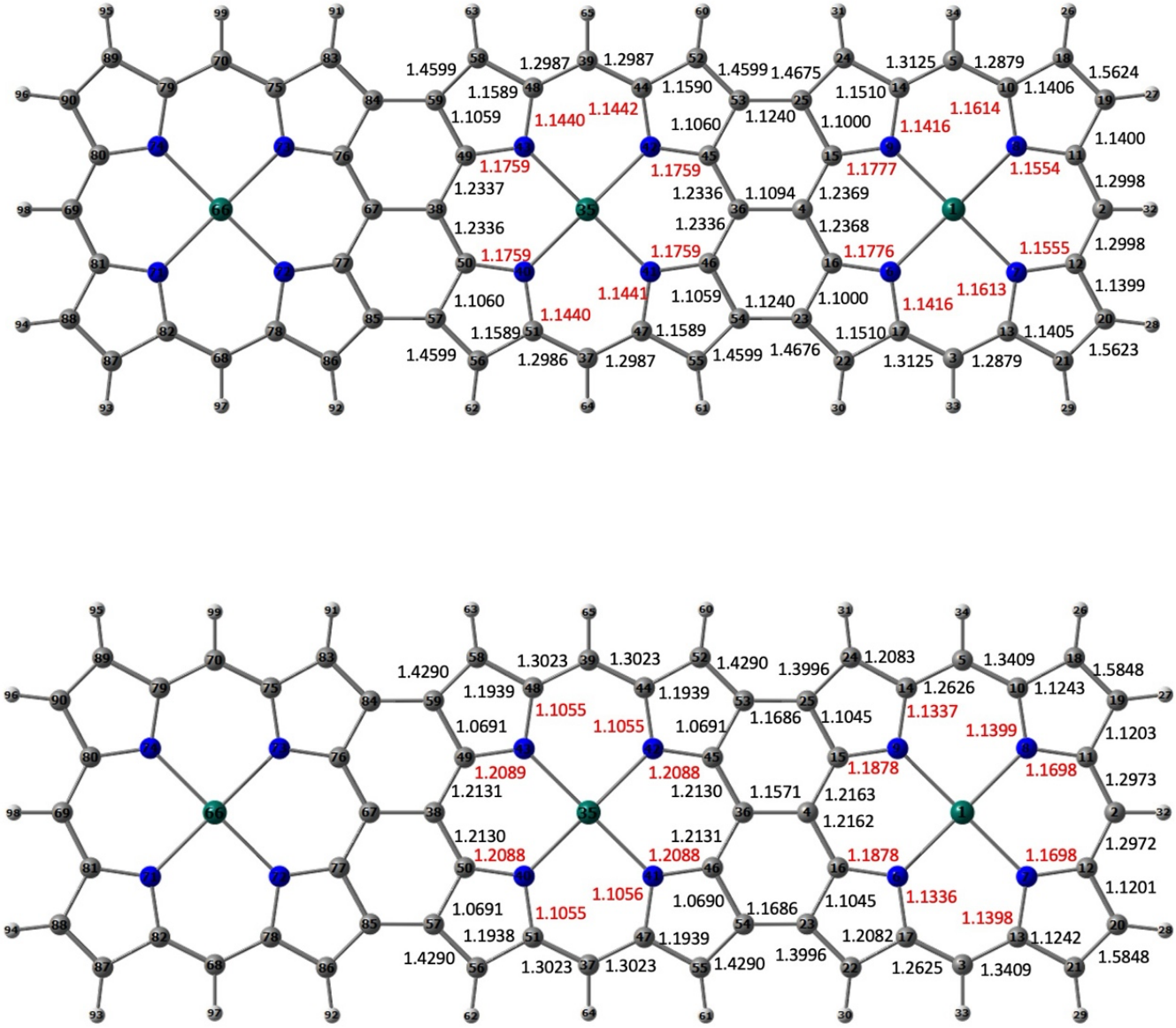


**Figure S10**. Delocalization indices for $PT_3$ in $S_0$ (top) and $T_1$ (bottom), computed at PBE0-D3/def2-TZVP. Inner bonds are highlighted in red.

**Table S3**. Aromaticity indices for the selected circuits for $PT_3$ in $S_0$.

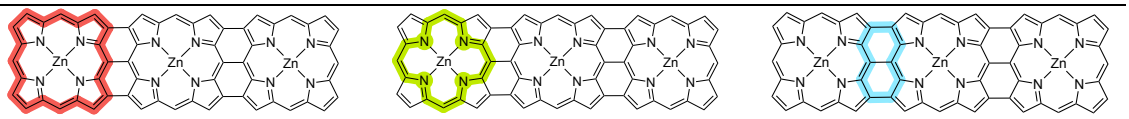

| | Ring circuit 1 | | Ring circuit 2 | | Ring circuit 3 | |
|---|---|---|---|---|---|---|
| | PBE0-D3 | ωB97X-D | PBE0-D3 | ωB97X-D | PBE0-D3 | ωB97X-D |
| FLU | 0.0201 | 0.0209 | 0.0047 | 0.0042 | 0.0336 | 0.0340 |
| HOMA | 0.7140 | 0.6850 | 0.9560 | 0.9605 | 0.6070 | 0.5771 |
| AV1245 | 1.5180 | 1.5470 | 0.9840 | 0.9890 | 0.2910 | 0.2660 |
| $AV_{min}$ | 0.1780 | 0.1980 | 0.5190 | 0.3940 | 0.1440 | 0.1040 |
| $EDDB_P$[a] | 4.5982 | | 8.4065 | | 1.5563 | |

[a]Computed at ωB97X-D/def2-TZVP

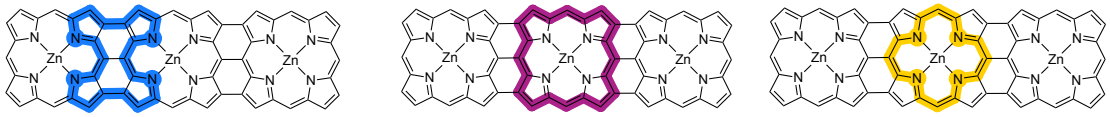

| | Ring circuit 4 | | Ring circuit 5 | | Ring circuit 6 | |
|---|---|---|---|---|---|---|
| | PBE0-D3 | ωB97X-D | PBE0-D3 | ωB97X-D | PBE0-D3 | ωB97X-D |
| FLU | 0.0131 | 0.0142 | 0.0203 | 0.0208 | 0.0061 | 0.0051 |
| HOMA | 0.8050 | 0.7626 | 0.7390 | 0.7145 | 0.9480 | 0.9571 |
| AV1245 | –0.7020 | -0.7120 | 1.3410 | 1.4050 | 0.9470 | 0.9410 |
| $AV_{min}$ | –8.0700 | -7.9790 | 0.1980 | 0.2460 | 0.6550 | 0.5050 |
| $EDDB_P$[a] | 5.2031 | | 5.6960 | | 8.5218 | |

[a]Computed at ωB97X-D/def2-TZVP

**Table S4**. Aromaticity indices for the selected circuits for $PT_3$ in $T_1$.

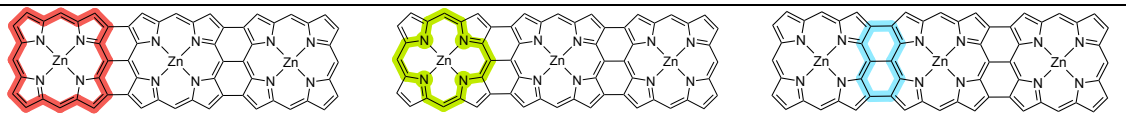

| | Ring circuit 1 | | Ring circuit 2 | | Ring circuit 3 | |
|---|---|---|---|---|---|---|
| | PBE0-D3 | ωB97X-D | PBE0-D3 | ωB97X-D | PBE0-D3 | ωB97X-D |
| FLU | 0.0203 | 0.0196 | 0.0056 | 0.0069 | 0.0354 | 0.0368 |
| HOMA | 0.7140 | 0.7295 | 0.9410 | 0.9158 | 0.5640 | 0.5641 |
| AV1245 | 1.3410 | 1.3940 | 0.8660 | 0.8660 | 0.2120 | 0.3740 |
| $AV_{min}$ | 0.0190 | 0.1260 | 0.2860 | 0.3850 | 0.0190 | 0.1000 |
| $EDDB_P$[a] | 5.8385 | | 4.8453 | | 2.3448 | |

[a]Computed at ωB97X-D/def2-TZVP

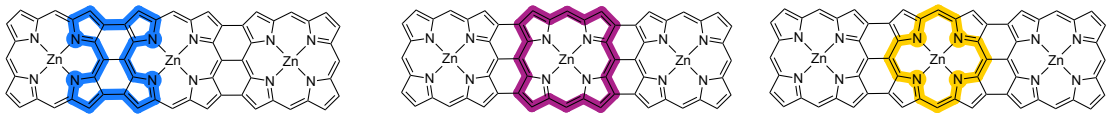

| | Ring circuit 4 | | Ring circuit 5 | | Ring circuit 6 | |
|---|---|---|---|---|---|---|
| | PBE0-D3 | ωB97X-D | PBE0-D3 | ωB97X-D | PBE0-D3 | ωB97X-D |
| FLU | 0.0110 | 0.0149 | 0.0218 | 0.0197 | 0.0083 | 0.0128 |
| HOMA | 0.8660 | 0.7858 | 0.6990 | 0.7740 | 0.9150 | 0.8251 |
| AV1245 | –0.5570 | -1.6240 | 0.9490 | 1.5120 | 0.9170 | 0.8840 |
| $AV_{min}$ | –8.2990 | -12.282 | 0.0000 | 0.1000 | 0.3780 | 0.2070 |
| $EDDB_P$[a] | 7.1025 | | 5.7973 | | 3.9886 | |

[a]Computed at ωB97X-D/def2-TZVP

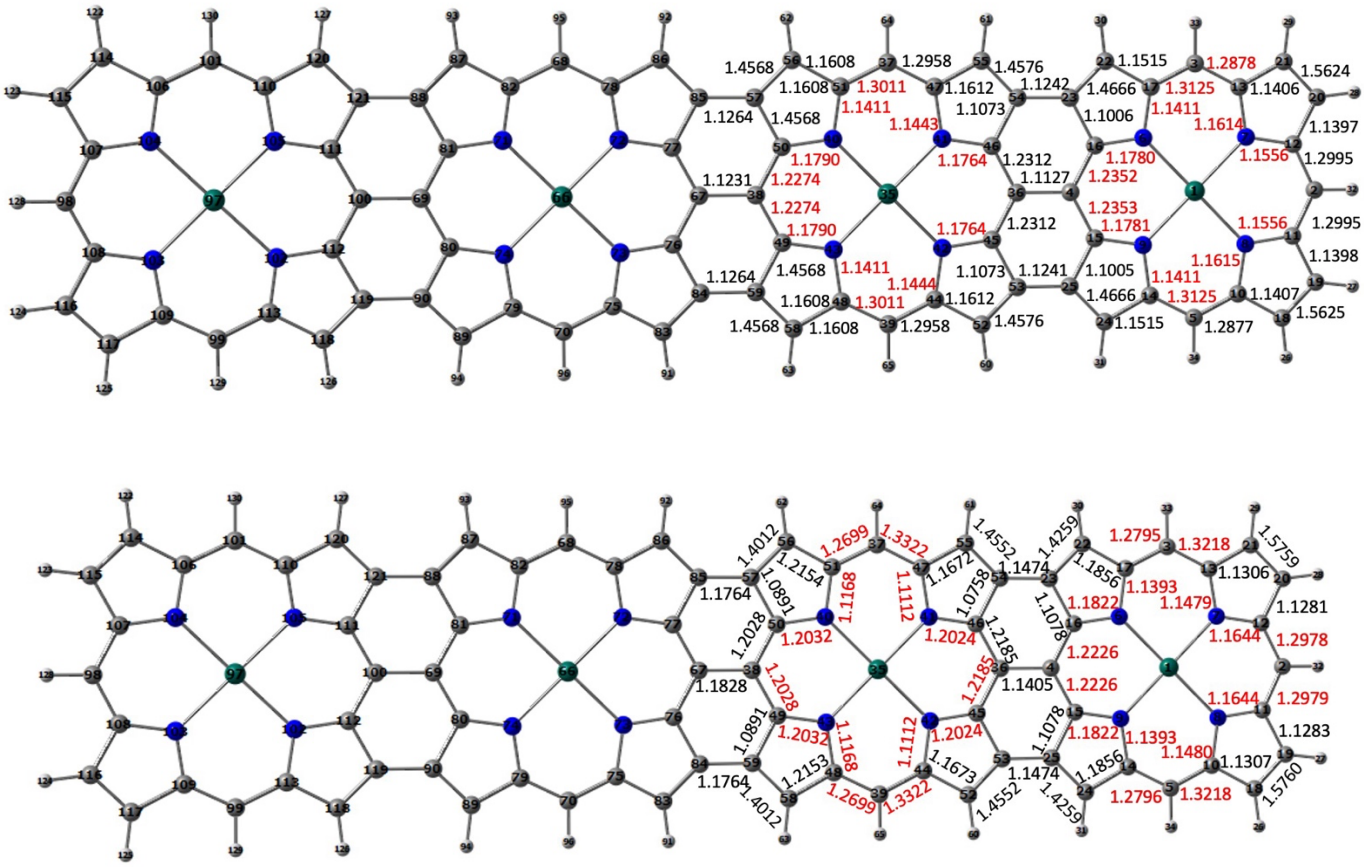

**Figure S11**. Delocalization indices for $PT_4$ in $S_0$ (top) and $T_1$ (bottom), computed at the PBE0-D3/def2-TZVP level of theory. Inner bonds are highlighted in red.

**Table S5**. Aromaticity indices for the selected circuits for $PT_4$ in $S_0$.

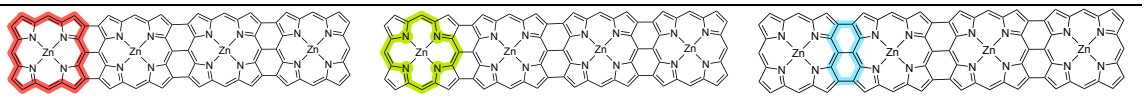

| | Ring circuit 1 | | Ring circuit 2 | | Ring circuit 3 | |
|---|---|---|---|---|---|---|
| | PBE0-D3 | ωB97X-D | PBE0-D3 | ωB97X-D | PBE0-D3 | ωB97X-D |
| FLU | 0.0205 | 0.0209 | 0.0057 | 0.0042 | 0.0332 | 0.0339 |
| HOMA | 0.5772 | 0.6826 | 0.8935 | 0.9602 | 0.3456 | 0.5794 |
| AV1245 | 1.5530 | 1.5420 | 1.0080 | 0.9950 | 0.3180 | 0.2700 |
| $AV_{min}$ | 0.1900 | 0.1930 | 0.5390 | 0.4010 | 0.1650 | 0.1020 |
| $EDDB_P$[a] | 4.8558 | | 8.4371 | | 1.5459 | |

[a]Computed at ωB97X-D/def2-TZVP

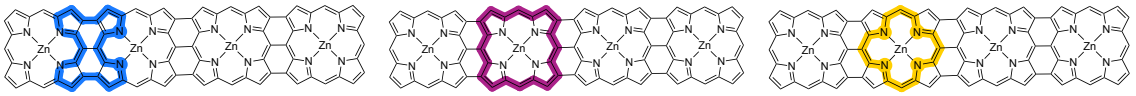

| | Ring circuit 4 | | Ring circuit 5 | | Ring circuit 6 | |
|---|---|---|---|---|---|---|
| | PBE0-D3 | ωB97X-D | PBE0-D3 | ωB97X-D | PBE0-D3 | ωB97X-D |
| FLU | 0.0136 | 0.0142 | 0.0205 | 0.0209 | 0.0071 | 0.0052 |
| HOMA | 0.6976 | 0.7628 | 0.5853 | 0.7123 | 0.8686 | 0.9568 |
| AV1245 | -0.8210 | -0.7140 | 1.3630 | 1.3960 | 0.9660 | 0.9440 |
| $AV_{min}$ | -8.8050 | -8.0210 | 0.1990 | 0.2280 | 0.7060 | 0.5120 |
| $EDDB_P$[a] | 5.1192 | | 5.5154 | | 8.4810 | |

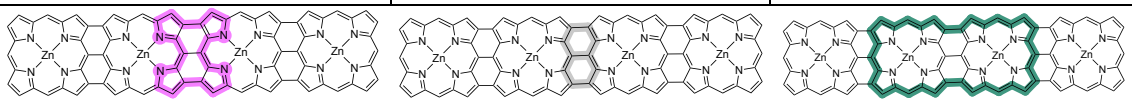

| | Ring circuit 7 | | Ring circuit 8 | | Ring circuit 9 | |
|---|---|---|---|---|---|---|
| | PBE0-D3 | ωB97X-D | PBE0-D3 | ωB97X-D | PBE0-D3 | ωB97X-D |
| FLU | 0.0135 | 0.0141 | 0.0332 | 0.0339 | 0.0187 | 0.0198 |
| HOMA | 0.7013 | 0.7669 | 0.3462 | 0.5823 | 0.6172 | 0.7066 |
| AV1245 | -0.8710 | -0.7460 | 0.3280 | 0.2790 | 1.2210 | 1.1710 |
| $AV_{min}$ | -8.9650 | -8.1110 | 0.1840 | 0.1230 | 0.2150 | 0.2690 |
| $EDDB_P$[a] | 5.6305 | | 1.6277 | | 6.0228 | |

[a]Computed at ωB97X-D/def2-TZVP

**Table S6**. Aromaticity indices for the selected circuits for $PT_4$ in $T_1$.

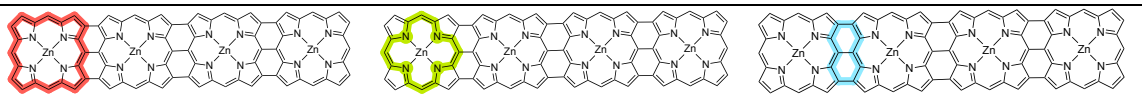

| | Ring circuit 1 | | Ring circuit 2 | | Ring circuit 3 | |
|---|---|---|---|---|---|---|
| | PBE0-D3 | ωB97X-D | PBE0-D3 | ωB97X-D | PBE0-D3 | ωB97X-D |
| FLU | 0.0201 | 0.0198 | 0.0067 | 0.0059 | 0.0345 | 0.0354 |
| HOMA | 0.5891 | 0.7219 | 0.8714 | 0.9347 | 0.3300 | 0.59201 |
| AV1245 | 1.5010 | 1.4210 | 0.9870 | 0.8920 | 0.3530 | 0.3760 |
| $AV_{min}$ | 0.1480 | 0.1510 | 0.6590 | 0.5190 | 0.1480 | 0.1400 |
| $EDDB_P$[a] | 6.0053 | | 5.9444 | | 2.1435 | |

[a]Computed at ωB97X-D/def2-TZVP

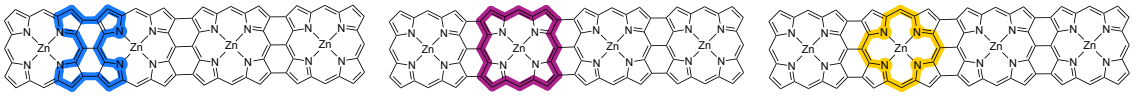

| | Ring circuit 4 | | Ring circuit 5 | | Ring circuit 6 | |
|---|---|---|---|---|---|---|
| | PBE0-D3 | ωB97X-D | PBE0-D3 | ωB97X-D | PBE0-D3 | ωB97X-D |
| FLU | 0.0137 | 0.0142 | 0.0202 | 0.0198 | 0.0106 | 0.0120 |
| HOMA | 0.7028 | 0.7920 | 0.6044 | 0.7672 | 0.7928 | 0.8390 |
| AV1245 | -1.1770 | -1.3380 | 1.3760 | 1.4040 | 0.9380 | 0.8620 |
| $AV_{min}$ | -10.4340 | -11.109 | 0.1120 | 0.0660 | 0.4140 | 0.2210 |
| $EDDB_P$[a] | 6.7012 | | 5.0012 | | 3.4694 | |

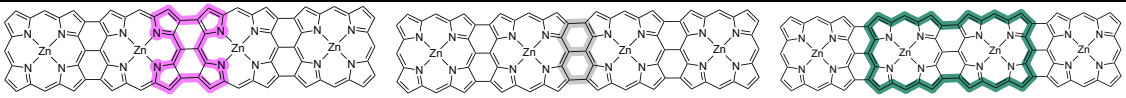

| | Ring circuit 7 | | Ring circuit 8 | | Ring circuit 9 | |
|---|---|---|---|---|---|---|
| | PBE0-D3 | ωB97X-D | PBE0-D3 | ωB97X-D | PBE0-D3 | ωB97X-D |
| FLU | 0.0142 | 0.0157 | 0.0360 | 0.0383 | 0.0164 | 0.0163 |
| HOMA | 0.6958 | 0.7731 | 0.2992 | 0.5253 | 0.6717 | 0.8154 |
| AV1245 | -1.486 | -1.8950 | 0.3490 | 0.3660 | 1.3690 | 1.3560 |
| $AV_{min}$ | -11.168 | -12.3950 | 0.1120 | 0.0900 | 0.1520 | 0.1400 |
| $EDDB_P$[a] | 6.2414 | | 2.4612 | | 10.1351 | |

[a]Computed at ωB97X-D/def2-TZVP

## Correlation between $AV_{min}$ and $EDDB_P$

Figure S10 displays the linear correlation between $AV_{min}$ and $EDDB_P$ indices for the $S_0$ state across the different evaluated ring circuits. The data, computed at the ωB97X-D/def2-TZVP level, are taken from Tables S1, S3, and S5, with the color code matching that used in the referenced tables. This analysis directly addresses the relationship between $AV_{min}$, which reflects the bottleneck of a given conjugation pathway, and EDDBP, which quantifies the number of cyclically delocalized electrons per atom that can coherently participate in the ring current. A good linear correlation is observed between both descriptors ($R^2$ = 0.8866)

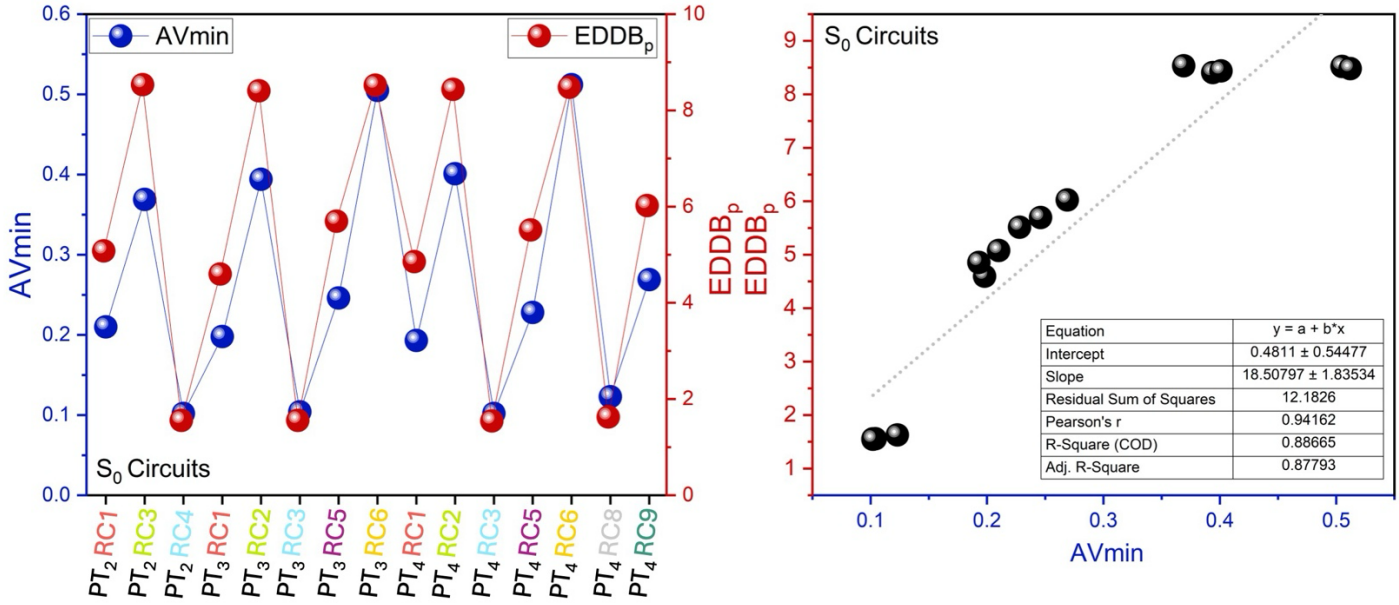


**Figure S12**. Correlation between $AV_{min}$ and $EDDB_P$ for $S_0$ considering the different ring circuits collected in Tables S1, S3 and S5, computed at ωB97X-D /def2-TZVP. The colors of the different circuits correspond to those shown in the referenced tables. Note that any circuit exhibiting negative $AV_{min}$ values were excluded from the correlation.

## Correlation between PBE0-D3 and ωB97X-D

Figures S11 and S12 shows the correlation between the $RCS_{net}$ values obtained with the ωB97X-D and PBE0-D3 functionals for the different evaluated ring circuits. Both functionals consistently capture the variations in $RCS_{net}$ across the different ring circuits, independently of the size of the tape porphyrin, as reflected by the linear correlation ($R^2$ = 0.9867). Figure S12 also presents the analogous correlation for the $BDDB_H$ values, also revealing an excellent agreement between both functionals ($R^2$ = 0.9994).

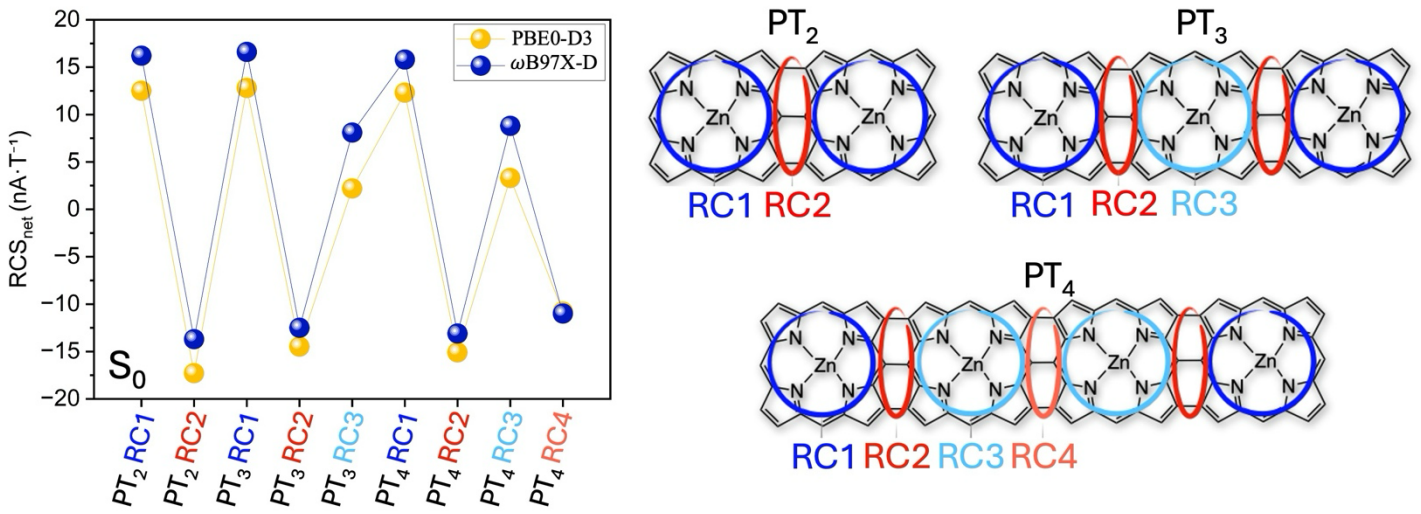


**Figure S13**. Comparison of the π-component ring-current strengths (nA·T$^{-1}$) for $S_0$ computed at ωB97X-D /def2-TZVP and PBE0-D3/def2-TZVP levels of theory.

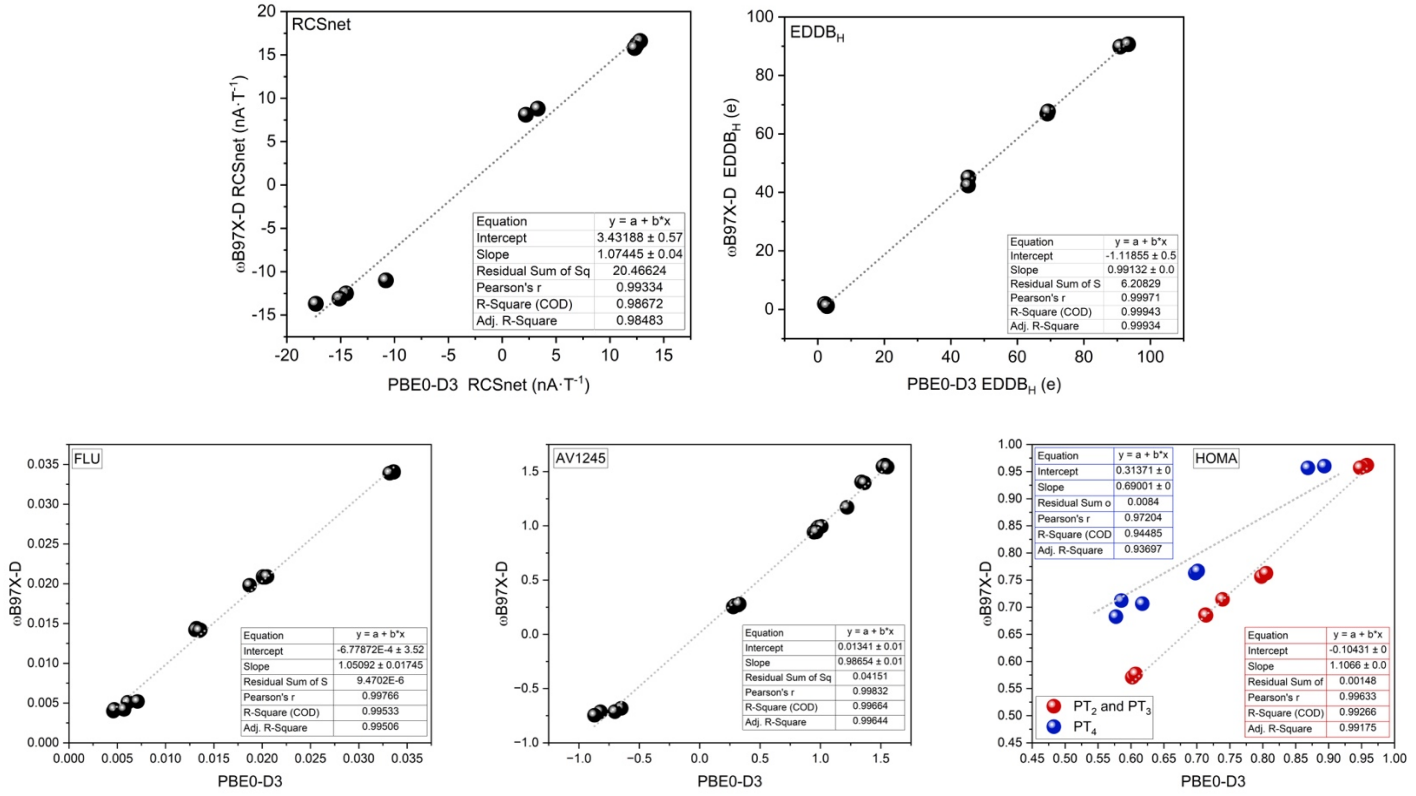


**Figure S14**. Linear regression between the ωB97X-D and PBE0-D3 results for the RCS$_{net}$ (left) and EDDB$_H$ (right) values in the $S_0$ state.

## Cartesian Coordinates

Cartesian coordinates of the PT2, PT3 and PT4 systems calculated at the ωB97X–D/def2–TZVP level of theory. The lowest frequencies (in $cm^{-1}$) and $T_1$–diagnostic values are show.

| [Zn-Porphyrin]$_2$ ($S_0$); $\upsilon_{min}$ = 21.9; $T_1$-diag = 0.0191 | | | |
|---|---|---|---|
| Zn | 0.000000000000 | 0.000000000000 | 4.195114000000 |
| C | 0.000000000000 | 3.405183000000 | 4.182018000000 |
| C | 0.000000000000 | 0.000000000000 | 0.739421000000 |
| C | 0.000000000000 | -3.405183000000 | 4.182018000000 |
| C | 0.000000000000 | 0.000000000000 | 7.601792000000 |
| N | 0.000000000000 | -1.429564000000 | 2.748644000000 |
| N | 0.000000000000 | 1.429564000000 | 2.748644000000 |
| N | 0.000000000000 | 1.442773000000 | 5.633606000000 |
| N | 0.000000000000 | -1.442773000000 | 5.633606000000 |
| C | 0.000000000000 | 1.241440000000 | 6.980100000000 |
| C | 0.000000000000 | 2.785979000000 | 5.428386000000 |
| C | 0.000000000000 | 2.781153000000 | 2.945445000000 |
| C | 0.000000000000 | 1.228386000000 | 1.409816000000 |
| C | 0.000000000000 | -1.241440000000 | 6.980100000000 |
| C | 0.000000000000 | -2.785979000000 | 5.428386000000 |
| C | 0.000000000000 | -2.781153000000 | 2.945445000000 |
| C | 0.000000000000 | -1.228386000000 | 1.409816000000 |
| C | 0.000000000000 | 2.511070000000 | 7.654670000000 |
| C | 0.000000000000 | 3.466509000000 | 6.694698000000 |
| C | 0.000000000000 | 3.457642000000 | 1.677205000000 |
| C | 0.000000000000 | 2.492411000000 | 0.719537000000 |
| C | 0.000000000000 | -2.492411000000 | 0.719537000000 |
| C | 0.000000000000 | -3.457642000000 | 1.677205000000 |
| C | 0.000000000000 | -2.511070000000 | 7.654670000000 |
| C | 0.000000000000 | -3.466509000000 | 6.694698000000 |
| H | 0.000000000000 | 2.643818000000 | 8.725428000000 |
| H | 0.000000000000 | 4.537882000000 | 6.822416000000 |
| H | 0.000000000000 | 4.528570000000 | 1.545038000000 |
| H | 0.000000000000 | -4.528570000000 | 1.545038000000 |
| H | 0.000000000000 | -2.643818000000 | 8.725428000000 |
| H | 0.000000000000 | -4.537882000000 | 6.822416000000 |
| H | 0.000000000000 | 4.488095000000 | 4.179276000000 |
| H | 0.000000000000 | -4.488095000000 | 4.179276000000 |
| H | 0.000000000000 | 0.000000000000 | 8.684761000000 |
| Zn | 0.000000000000 | 0.000000000000 | -4.195114000000 |
| C | 0.000000000000 | 3.405183000000 | -4.182018000000 |
| C | 0.000000000000 | 0.000000000000 | -7.601792000000 |
| C | 0.000000000000 | -3.405183000000 | -4.182018000000 |
| C | 0.000000000000 | 0.000000000000 | -0.739421000000 |
| N | 0.000000000000 | -1.442773000000 | -5.633606000000 |
| N | 0.000000000000 | 1.442773000000 | -5.633606000000 |
| N | 0.000000000000 | 1.429564000000 | -2.748644000000 |
| N | 0.000000000000 | -1.429564000000 | -2.748644000000 |
| C | 0.000000000000 | 1.228386000000 | -1.409816000000 |
| C | 0.000000000000 | 2.781153000000 | -2.945445000000 |
| C | 0.000000000000 | 2.785979000000 | -5.428386000000 |
| C | 0.000000000000 | 1.241440000000 | -6.980100000000 |
| C | 0.000000000000 | -1.228386000000 | -1.409816000000 |
| C | 0.000000000000 | -2.781153000000 | -2.945445000000 |
| C | 0.000000000000 | -2.785979000000 | -5.428386000000 |
| C | 0.000000000000 | -1.241440000000 | -6.980100000000 |
| C | 0.000000000000 | 2.492411000000 | -0.719537000000 |
| C | 0.000000000000 | 3.457642000000 | -1.677205000000 |
| C | 0.000000000000 | 3.466509000000 | -6.694698000000 |
| C | 0.000000000000 | 2.511070000000 | -7.654670000000 |
| C | 0.000000000000 | -2.511070000000 | -7.654670000000 |
| C | 0.000000000000 | -3.466509000000 | -6.694698000000 |
| C | 0.000000000000 | -2.492411000000 | -0.719537000000 |

| [Zn-Porphyrin]$_2$ ($T_1$); $\upsilon_{min}$ = 21.6; $T_1$-diag = 0.0199 | | | |
|---|---|---|---|
| Zn | 0.000000000000 | 4.177159000000 | 0.000004000000 |
| C | 0.000000000000 | 4.191816000000 | 3.417314000000 |
| C | 0.000000000000 | 0.721419000000 | -0.000069000000 |
| C | 0.000000000000 | 4.191746000000 | -3.417294000000 |
| C | 0.000000000000 | 7.592070000000 | 0.000003000000 |
| N | 0.000000000000 | 2.731917000000 | -1.436562000000 |
| N | 0.000000000000 | 2.731916000000 | 1.436479000000 |
| N | 0.000000000000 | 5.621212000000 | 1.435402000000 |
| N | 0.000000000000 | 5.621205000000 | -1.435279000000 |
| C | 0.000000000000 | 6.954285000000 | 1.236247000000 |
| C | 0.000000000000 | 5.408316000000 | 2.797207000000 |
| C | 0.000000000000 | 2.921255000000 | 2.798073000000 |
| C | 0.000000000000 | 1.398278000000 | 1.235019000000 |
| C | 0.000000000000 | 6.954383000000 | -1.236049000000 |
| C | 0.000000000000 | 5.408375000000 | -2.797001000000 |
| C | 0.000000000000 | 2.921326000000 | -2.798179000000 |
| C | 0.000000000000 | 1.398314000000 | -1.235234000000 |
| C | 0.000000000000 | 7.640120000000 | 2.520276000000 |
| C | 0.000000000000 | 6.692070000000 | 3.472734000000 |
| C | 0.000000000000 | 1.687586000000 | 3.475271000000 |
| C | 0.000000000000 | 0.706443000000 | 2.500789000000 |
| C | 0.000000000000 | 0.706494000000 | -2.501131000000 |
| C | 0.000000000000 | 1.687511000000 | -3.475483000000 |
| C | 0.000000000000 | 7.640234000000 | -2.520082000000 |
| C | 0.000000000000 | 6.692171000000 | -3.472512000000 |
| H | 0.000000000000 | 8.711900000000 | 2.644410000000 |
| H | 0.000000000000 | 6.822517000000 | 4.543981000000 |
| H | 0.000000000000 | 1.559178000000 | 4.545894000000 |
| H | 0.000000000000 | 1.559103000000 | -4.546103000000 |
| H | 0.000000000000 | 8.712013000000 | -2.644230000000 |
| H | 0.000000000000 | 6.822621000000 | -4.543758000000 |
| H | 0.000000000000 | 4.194616000000 | 4.500214000000 |
| H | 0.000000000000 | 4.194556000000 | -4.500191000000 |
| H | 0.000000000000 | 8.673579000000 | -0.000013000000 |
| Zn | 0.000000000000 | -4.177159000000 | 0.000004000000 |
| C | 0.000000000000 | -4.191816000000 | 3.417314000000 |
| C | 0.000000000000 | -7.592070000000 | 0.000003000000 |
| C | 0.000000000000 | -4.191746000000 | -3.417294000000 |
| C | 0.000000000000 | -0.721419000000 | -0.000069000000 |
| N | 0.000000000000 | -5.621205000000 | -1.435279000000 |
| N | 0.000000000000 | -5.621212000000 | 1.435402000000 |
| N | 0.000000000000 | -2.731916000000 | 1.436479000000 |
| N | 0.000000000000 | -2.731917000000 | -1.436562000000 |
| C | 0.000000000000 | -1.398278000000 | 1.235019000000 |
| C | 0.000000000000 | -2.921255000000 | 2.798073000000 |
| C | 0.000000000000 | -5.408316000000 | 2.797207000000 |
| C | 0.000000000000 | -6.954285000000 | 1.236247000000 |
| C | 0.000000000000 | -1.398314000000 | -1.235234000000 |
| C | 0.000000000000 | -2.921326000000 | -2.798179000000 |
| C | 0.000000000000 | -5.408375000000 | -2.797001000000 |
| C | 0.000000000000 | -6.954383000000 | -1.236049000000 |
| C | 0.000000000000 | -0.706443000000 | 2.500789000000 |
| C | 0.000000000000 | -1.687586000000 | 3.475271000000 |
| C | 0.000000000000 | -6.692070000000 | 3.472734000000 |
| C | 0.000000000000 | -7.640120000000 | 2.520276000000 |
| C | 0.000000000000 | -7.640234000000 | -2.520082000000 |
| C | 0.000000000000 | -6.692171000000 | -3.472512000000 |
| C | 0.000000000000 | -0.706494000000 | -2.501131000000 |

| | | | |
|---|---|---|---|
| C | 0.000000000000 | -3.457642000000 | -1.677205000000 |
| H | 0.000000000000 | 4.528570000000 | -1.545038000000 |
| H | 0.000000000000 | 4.537882000000 | -6.822416000000 |
| H | 0.000000000000 | 2.643818000000 | -8.725428000000 |
| H | 0.000000000000 | -2.643818000000 | -8.725428000000 |
| H | 0.000000000000 | -4.537882000000 | -6.822416000000 |
| H | 0.000000000000 | -4.528570000000 | -1.545038000000 |
| H | 0.000000000000 | 4.488095000000 | -4.179276000000 |
| H | 0.000000000000 | 0.000000000000 | -8.684761000000 |
| H | 0.000000000000 | -4.488095000000 | -4.179276000000 |

| | | | |
|---|---|---|---|
| C | 0.000000000000 | -1.687511000000 | -3.475483000000 |
| H | 0.000000000000 | -1.559178000000 | 4.545894000000 |
| H | 0.000000000000 | -6.822517000000 | 4.543981000000 |
| H | 0.000000000000 | -8.711900000000 | 2.644410000000 |
| H | 0.000000000000 | -8.712013000000 | -2.644230000000 |
| H | 0.000000000000 | -6.822621000000 | -4.543758000000 |
| H | 0.000000000000 | -1.559103000000 | -4.546103000000 |
| H | 0.000000000000 | -4.194616000000 | 4.500214000000 |
| H | 0.000000000000 | -8.673579000000 | -0.000013000000 |
| H | 0.000000000000 | -4.194556000000 | -4.500191000000 |

[Zn-Porphyrin]$_3$ ($S_0$); $\upsilon_{min}$ = 9.0; $T_1$-diag = 0.0129

| | | | |
|---|---|---|---|
| Zn | 0.000000000000 | 0.000000000000 | 8.382268000000 |
| C | 0.000000000000 | 0.000000000000 | 11.789524000000 |
| C | 0.000000000000 | 3.405269000000 | 8.368982000000 |
| C | 0.000000000000 | 0.000000000000 | 4.927574000000 |
| C | 0.000000000000 | -3.405269000000 | 8.368982000000 |
| N | 0.000000000000 | 1.429610000000 | 6.936340000000 |
| N | 0.000000000000 | 1.443103000000 | 9.821505000000 |
| N | 0.000000000000 | -1.443103000000 | 9.821505000000 |
| N | 0.000000000000 | -1.429610000000 | 6.936340000000 |
| C | 0.000000000000 | -2.785638000000 | 9.616805000000 |
| C | 0.000000000000 | -1.241716000000 | 11.168405000000 |
| C | 0.000000000000 | 1.241716000000 | 11.168405000000 |
| C | 0.000000000000 | 2.785638000000 | 9.616805000000 |
| C | 0.000000000000 | -2.782019000000 | 7.133661000000 |
| C | 0.000000000000 | -1.229127000000 | 5.598236000000 |
| C | 0.000000000000 | 1.229127000000 | 5.598236000000 |
| C | 0.000000000000 | 2.782019000000 | 7.133661000000 |
| C | 0.000000000000 | -3.466345000000 | 10.882327000000 |
| C | 0.000000000000 | -2.510736000000 | 11.842748000000 |
| C | 0.000000000000 | 2.510736000000 | 11.842748000000 |
| C | 0.000000000000 | 3.466345000000 | 10.882327000000 |
| C | 0.000000000000 | 3.458603000000 | 5.864895000000 |
| C | 0.000000000000 | 2.493746000000 | 4.907286000000 |
| C | 0.000000000000 | -3.458603000000 | 5.864895000000 |
| C | 0.000000000000 | -2.493746000000 | 4.907286000000 |
| H | 0.000000000000 | -4.537709000000 | 11.009908000000 |
| H | 0.000000000000 | -2.643681000000 | 12.913462000000 |
| H | 0.000000000000 | 2.643681000000 | 12.913462000000 |
| H | 0.000000000000 | 4.537709000000 | 11.009908000000 |
| H | 0.000000000000 | 4.529522000000 | 5.732767000000 |
| H | 0.000000000000 | -4.529522000000 | 5.732767000000 |
| H | 0.000000000000 | 0.000000000000 | 12.872527000000 |
| H | 0.000000000000 | 4.488184000000 | 8.366495000000 |
| H | 0.000000000000 | -4.488184000000 | 8.366495000000 |
| Zn | 0.000000000000 | 0.000000000000 | 0.000000000000 |
| C | 0.000000000000 | 0.000000000000 | 3.451546000000 |
| C | 0.000000000000 | 3.400141000000 | 0.000000000000 |
| C | 0.000000000000 | 0.000000000000 | -3.451546000000 |
| C | 0.000000000000 | -3.400141000000 | 0.000000000000 |
| N | 0.000000000000 | 1.429952000000 | -1.441896000000 |
| N | 0.000000000000 | 1.429952000000 | 1.441896000000 |
| N | 0.000000000000 | -1.429952000000 | 1.441896000000 |
| N | 0.000000000000 | -1.429952000000 | -1.441896000000 |
| C | 0.000000000000 | -2.780048000000 | 1.242935000000 |
| C | 0.000000000000 | -1.230127000000 | 2.781031000000 |
| C | 0.000000000000 | 1.230127000000 | 2.781031000000 |
| C | 0.000000000000 | 2.780048000000 | 1.242935000000 |
| C | 0.000000000000 | -2.780048000000 | -1.242935000000 |
| C | 0.000000000000 | -1.230127000000 | -2.781031000000 |
| C | 0.000000000000 | 1.230127000000 | -2.781031000000 |
| C | 0.000000000000 | 2.780048000000 | -1.242935000000 |
| C | 0.000000000000 | -3.458180000000 | 2.507591000000 |
| C | 0.000000000000 | -2.492970000000 | 3.468356000000 |
| C | 0.000000000000 | 2.492970000000 | 3.468356000000 |
| C | 0.000000000000 | 3.458180000000 | 2.507591000000 |
| C | 0.000000000000 | 3.458180000000 | -2.507591000000 |

[Zn-Porphyrin]$_3$ ($T_1$); $\upsilon_{min}$ = 9.3; $T_1$-diag = 0.0187

| | | | |
|---|---|---|---|
| Zn | 0.000000000000 | 0.000000000000 | 8.362332000000 |
| C | 0.000000000000 | 0.000000000000 | 11.783658000000 |
| C | 0.000000000000 | 3.406734000000 | 8.363998000000 |
| C | 0.000000000000 | 0.000000000000 | 4.894045000000 |
| C | 0.000000000000 | -3.406734000000 | 8.363998000000 |
| N | 0.000000000000 | 1.434340000000 | 6.916628000000 |
| N | 0.000000000000 | 1.443029000000 | 9.814349000000 |
| N | 0.000000000000 | -1.443029000000 | 9.814349000000 |
| N | 0.000000000000 | -1.434340000000 | 6.916628000000 |
| C | 0.000000000000 | -2.788700000000 | 9.609683000000 |
| C | 0.000000000000 | -1.244999000000 | 11.158962000000 |
| C | 0.000000000000 | 1.244999000000 | 11.158962000000 |
| C | 0.000000000000 | 2.788700000000 | 9.609683000000 |
| C | 0.000000000000 | -2.793702000000 | 7.119805000000 |
| C | 0.000000000000 | -1.248349000000 | 5.582468000000 |
| C | 0.000000000000 | 1.248349000000 | 5.582468000000 |
| C | 0.000000000000 | 2.793702000000 | 7.119805000000 |
| C | 0.000000000000 | -3.468732000000 | 10.873867000000 |
| C | 0.000000000000 | -2.512207000000 | 11.834896000000 |
| C | 0.000000000000 | 2.512207000000 | 11.834896000000 |
| C | 0.000000000000 | 3.468732000000 | 10.873867000000 |
| C | 0.000000000000 | 3.473427000000 | 5.867938000000 |
| C | 0.000000000000 | 2.504538000000 | 4.897516000000 |
| C | 0.000000000000 | -3.473427000000 | 5.867938000000 |
| C | 0.000000000000 | -2.504538000000 | 4.897516000000 |
| H | 0.000000000000 | -4.540209000000 | 11.001262000000 |
| H | 0.000000000000 | -2.643926000000 | 12.905720000000 |
| H | 0.000000000000 | 2.643926000000 | 12.905720000000 |
| H | 0.000000000000 | 4.540209000000 | 11.001262000000 |
| H | 0.000000000000 | 4.544648000000 | 5.739882000000 |
| H | 0.000000000000 | -4.544648000000 | 5.739882000000 |
| H | 0.000000000000 | 0.000000000000 | 12.866479000000 |
| H | 0.000000000000 | 4.490120000000 | 8.365512000000 |
| H | 0.000000000000 | -4.490120000000 | 8.365512000000 |
| Zn | 0.000000000000 | 0.000000000000 | 0.000000000000 |
| C | 0.000000000000 | 0.000000000000 | 3.476319000000 |
| C | 0.000000000000 | 3.402328000000 | 0.000000000000 |
| C | 0.000000000000 | 0.000000000000 | -3.476319000000 |
| C | 0.000000000000 | -3.402328000000 | 0.000000000000 |
| N | 0.000000000000 | 1.434151000000 | -1.454244000000 |
| N | 0.000000000000 | 1.434151000000 | 1.454244000000 |
| N | 0.000000000000 | -1.434151000000 | 1.454244000000 |
| N | 0.000000000000 | -1.434151000000 | -1.454244000000 |
| C | 0.000000000000 | -2.797819000000 | 1.249585000000 |
| C | 0.000000000000 | -1.253265000000 | 2.783087000000 |
| C | 0.000000000000 | 1.253265000000 | 2.783087000000 |
| C | 0.000000000000 | 2.797819000000 | 1.249585000000 |
| C | 0.000000000000 | -2.797819000000 | -1.249585000000 |
| C | 0.000000000000 | -1.253265000000 | -2.783087000000 |
| C | 0.000000000000 | 1.253265000000 | -2.783087000000 |
| C | 0.000000000000 | 2.797819000000 | -1.249585000000 |
| C | 0.000000000000 | -3.476246000000 | 2.492947000000 |
| C | 0.000000000000 | -2.504865000000 | 3.467271000000 |
| C | 0.000000000000 | 2.504865000000 | 3.467271000000 |
| C | 0.000000000000 | 3.476246000000 | 2.492947000000 |
| C | 0.000000000000 | 3.476246000000 | -2.492947000000 |

| | | | |
|---|---|---|---|
| C | 0.000000000000 | 2.492970000000 | -3.468356000000 |
| C | 0.000000000000 | -3.458180000000 | -2.507591000000 |
| C | 0.000000000000 | -2.492970000000 | -3.468356000000 |
| H | 0.000000000000 | -4.529246000000 | 2.638614000000 |
| H | 0.000000000000 | 4.529246000000 | 2.638614000000 |
| H | 0.000000000000 | 4.529246000000 | -2.638614000000 |
| H | 0.000000000000 | -4.529246000000 | -2.638614000000 |
| H | 0.000000000000 | 4.483167000000 | 0.000000000000 |
| H | 0.000000000000 | -4.483167000000 | 0.000000000000 |
| Zn | 0.000000000000 | 0.000000000000 | -8.382268000000 |
| C | 0.000000000000 | 0.000000000000 | -4.927574000000 |
| C | 0.000000000000 | 3.405269000000 | -8.368982000000 |
| C | 0.000000000000 | 0.000000000000 | -11.789524000000 |
| C | 0.000000000000 | -3.405269000000 | -8.368982000000 |
| N | 0.000000000000 | 1.443103000000 | -9.821505000000 |
| N | 0.000000000000 | 1.429610000000 | -6.936340000000 |
| N | 0.000000000000 | -1.429610000000 | -6.936340000000 |
| N | 0.000000000000 | -1.443103000000 | -9.821505000000 |
| C | 0.000000000000 | -2.782019000000 | -7.133661000000 |
| C | 0.000000000000 | -1.229127000000 | -5.598236000000 |
| C | 0.000000000000 | 1.229127000000 | -5.598236000000 |
| C | 0.000000000000 | 2.782019000000 | -7.133661000000 |
| C | 0.000000000000 | -2.785638000000 | -9.616805000000 |
| C | 0.000000000000 | -1.241716000000 | -11.168405000000 |
| C | 0.000000000000 | 1.241716000000 | -11.168405000000 |
| C | 0.000000000000 | 2.785638000000 | -9.616805000000 |
| C | 0.000000000000 | -3.458603000000 | -5.864895000000 |
| C | 0.000000000000 | -2.493746000000 | -4.907286000000 |
| C | 0.000000000000 | 2.493746000000 | -4.907286000000 |
| C | 0.000000000000 | 3.458603000000 | -5.864895000000 |
| C | 0.000000000000 | 3.466345000000 | -10.882327000000 |
| C | 0.000000000000 | 2.510736000000 | -11.842748000000 |
| C | 0.000000000000 | -3.466345000000 | -10.882327000000 |
| C | 0.000000000000 | -2.510736000000 | -11.842748000000 |
| H | 0.000000000000 | -4.529522000000 | -5.732767000000 |
| H | 0.000000000000 | 4.529522000000 | -5.732767000000 |
| H | 0.000000000000 | 4.537709000000 | -11.009908000000 |
| H | 0.000000000000 | 2.643681000000 | -12.913462000000 |
| H | 0.000000000000 | -4.537709000000 | -11.009908000000 |
| H | 0.000000000000 | -2.643681000000 | -12.913462000000 |
| H | 0.000000000000 | 4.488184000000 | -8.366495000000 |
| H | 0.000000000000 | 0.000000000000 | -12.872527000000 |
| H | 0.000000000000 | -4.488184000000 | -8.366495000000 |

| | | | |
|---|---|---|---|
| C | 0.000000000000 | 2.504865000000 | -3.467271000000 |
| C | 0.000000000000 | -3.476246000000 | -2.492947000000 |
| C | 0.000000000000 | -2.504865000000 | -3.467271000000 |
| H | 0.000000000000 | -4.547565000000 | 2.621220000000 |
| H | 0.000000000000 | 4.547565000000 | 2.621220000000 |
| H | 0.000000000000 | 4.547565000000 | -2.621220000000 |
| H | 0.000000000000 | -4.547565000000 | -2.621220000000 |
| H | 0.000000000000 | 4.486782000000 | 0.000000000000 |
| H | 0.000000000000 | -4.486782000000 | 0.000000000000 |
| Zn | 0.000000000000 | 0.000000000000 | -8.362332000000 |
| C | 0.000000000000 | 0.000000000000 | -4.894045000000 |
| C | 0.000000000000 | 3.406734000000 | -8.363998000000 |
| C | 0.000000000000 | 0.000000000000 | -11.783658000000 |
| C | 0.000000000000 | -3.406734000000 | -8.363998000000 |
| N | 0.000000000000 | 1.443029000000 | -9.814349000000 |
| N | 0.000000000000 | 1.434340000000 | -6.916628000000 |
| N | 0.000000000000 | -1.434340000000 | -6.916628000000 |
| N | 0.000000000000 | -1.443029000000 | -9.814349000000 |
| C | 0.000000000000 | -2.793702000000 | -7.119805000000 |
| C | 0.000000000000 | -1.248349000000 | -5.582468000000 |
| C | 0.000000000000 | 1.248349000000 | -5.582468000000 |
| C | 0.000000000000 | 2.793702000000 | -7.119805000000 |
| C | 0.000000000000 | -2.788700000000 | -9.609683000000 |
| C | 0.000000000000 | -1.244999000000 | -11.158962000000 |
| C | 0.000000000000 | 1.244999000000 | -11.158962000000 |
| C | 0.000000000000 | 2.788700000000 | -9.609683000000 |
| C | 0.000000000000 | -3.473427000000 | -5.867938000000 |
| C | 0.000000000000 | -2.504538000000 | -4.897516000000 |
| C | 0.000000000000 | 2.504538000000 | -4.897516000000 |
| C | 0.000000000000 | 3.473427000000 | -5.867938000000 |
| C | 0.000000000000 | 3.468732000000 | -10.873867000000 |
| C | 0.000000000000 | 2.512207000000 | -11.834896000000 |
| C | 0.000000000000 | -3.468732000000 | -10.873867000000 |
| C | 0.000000000000 | -2.512207000000 | -11.834896000000 |
| H | 0.000000000000 | -4.544648000000 | -5.739882000000 |
| H | 0.000000000000 | 4.544648000000 | -5.739882000000 |
| H | 0.000000000000 | 4.540209000000 | -11.001262000000 |
| H | 0.000000000000 | 2.643926000000 | -12.905720000000 |
| H | 0.000000000000 | -4.540209000000 | -11.001262000000 |
| H | 0.000000000000 | -2.643926000000 | -12.905720000000 |
| H | 0.000000000000 | 4.490120000000 | -8.365512000000 |
| H | 0.000000000000 | 0.000000000000 | -12.866479000000 |
| H | 0.000000000000 | -4.490120000000 | -8.365512000000 |

| [Zn-Porphyrin]$_4$ ($S_0$); $\upsilon_{min}$ = 5.2; $T_1$-diag = 0.0160 | | | |
|---|---|---|---|
| Zn | 0.000000000000 | 0.000000000000 | 12.569707000000 |
| C | 0.000000000000 | 0.000000000000 | 15.977162000000 |
| C | 0.000000000000 | 3.405425000000 | 12.556352000000 |
| C | 0.000000000000 | 0.000000000000 | 9.116103000000 |
| C | 0.000000000000 | -3.405425000000 | 12.556352000000 |
| N | 0.000000000000 | 1.429812000000 | 11.124319000000 |
| N | 0.000000000000 | 1.443528000000 | 14.009272000000 |
| N | 0.000000000000 | -1.443528000000 | 14.009272000000 |
| N | 0.000000000000 | -1.429812000000 | 11.124319000000 |
| C | 0.000000000000 | -2.785446000000 | 13.805047000000 |
| C | 0.000000000000 | -1.241904000000 | 15.356481000000 |
| C | 0.000000000000 | 1.241904000000 | 15.356481000000 |
| C | 0.000000000000 | 2.785446000000 | 13.805047000000 |
| C | 0.000000000000 | -2.782198000000 | 11.321964000000 |
| C | 0.000000000000 | -1.229281000000 | 9.786305000000 |
| C | 0.000000000000 | 1.229281000000 | 9.786305000000 |
| C | 0.000000000000 | 2.782198000000 | 11.321964000000 |
| C | 0.000000000000 | -3.466414000000 | 15.070106000000 |
| C | 0.000000000000 | -2.510520000000 | 16.030828000000 |
| C | 0.000000000000 | 2.510520000000 | 16.030828000000 |
| C | 0.000000000000 | 3.466414000000 | 15.070106000000 |
| C | 0.000000000000 | 3.459088000000 | 10.052357000000 |
| C | 0.000000000000 | 2.494380000000 | 9.095065000000 |

| [Zn-Porphyrin]$_4$ ($T_1$); $\upsilon_{min}$ = 5.3; $T_1$-diag = 0.0184 | | | |
|---|---|---|---|
| Zn | 0.000000000000 | 0.000000000000 | 12.550425000000 |
| C | 0.000000000000 | 0.000000000000 | 15.967595000000 |
| C | 0.000000000000 | 3.406246000000 | 12.547681000000 |
| C | 0.000000000000 | 0.000000000000 | 9.085790000000 |
| C | 0.000000000000 | -3.406246000000 | 12.547681000000 |
| N | 0.000000000000 | 1.432884000000 | 11.104713000000 |
| N | 0.000000000000 | 1.443141000000 | 13.998547000000 |
| N | 0.000000000000 | -1.443141000000 | 13.998547000000 |
| N | 0.000000000000 | -1.432884000000 | 11.104713000000 |
| C | 0.000000000000 | -2.787874000000 | 13.793814000000 |
| C | 0.000000000000 | -1.244179000000 | 15.343859000000 |
| C | 0.000000000000 | 1.244179000000 | 15.343859000000 |
| C | 0.000000000000 | 2.787874000000 | 13.793814000000 |
| C | 0.000000000000 | -2.789461000000 | 11.306099000000 |
| C | 0.000000000000 | -1.242540000000 | 9.768736000000 |
| C | 0.000000000000 | 1.242540000000 | 9.768736000000 |
| C | 0.000000000000 | 2.789461000000 | 11.306099000000 |
| C | 0.000000000000 | -3.468208000000 | 15.058660000000 |
| C | 0.000000000000 | -2.511999000000 | 16.019417000000 |
| C | 0.000000000000 | 2.511999000000 | 16.019417000000 |
| C | 0.000000000000 | 3.468208000000 | 15.058660000000 |
| C | 0.000000000000 | 3.468610000000 | 10.049008000000 |
| C | 0.000000000000 | 2.500906000000 | 9.082402000000 |

| | | | |
|---|---|---|---|
| C | 0.000000000000 | -3.459088000000 | 10.052357000000 |
| C | 0.000000000000 | -2.494380000000 | 9.095065000000 |
| H | 0.000000000000 | -4.537881000000 | 15.197414000000 |
| H | 0.000000000000 | -2.643308000000 | 17.101647000000 |
| H | 0.000000000000 | 2.643308000000 | 17.101647000000 |
| H | 0.000000000000 | 4.537881000000 | 15.197414000000 |
| H | 0.000000000000 | 4.530099000000 | 9.920765000000 |
| H | 0.000000000000 | -4.530099000000 | 9.920765000000 |
| H | 0.000000000000 | 0.000000000000 | 17.060277000000 |
| H | 0.000000000000 | 4.488377000000 | 12.554108000000 |
| H | 0.000000000000 | -4.488377000000 | 12.554108000000 |
| Zn | 0.000000000000 | 0.000000000000 | 4.186783000000 |
| C | 0.000000000000 | 0.000000000000 | 7.639528000000 |
| C | 0.000000000000 | 3.400567000000 | 4.186717000000 |
| C | 0.000000000000 | 0.000000000000 | 0.737158000000 |
| C | 0.000000000000 | -3.400567000000 | 4.186717000000 |
| N | 0.000000000000 | 1.430498000000 | 2.745983000000 |
| N | 0.000000000000 | 1.430766000000 | 5.629787000000 |
| N | 0.000000000000 | -1.430766000000 | 5.629787000000 |
| N | 0.000000000000 | -1.430498000000 | 2.745983000000 |
| C | 0.000000000000 | -2.779597000000 | 5.431213000000 |
| C | 0.000000000000 | -1.230637000000 | 6.969873000000 |
| C | 0.000000000000 | 1.230637000000 | 6.969873000000 |
| C | 0.000000000000 | 2.779597000000 | 5.431213000000 |
| C | 0.000000000000 | -2.780938000000 | 2.945506000000 |
| C | 0.000000000000 | -1.230973000000 | 1.407112000000 |
| C | 0.000000000000 | 1.230973000000 | 1.407112000000 |
| C | 0.000000000000 | 2.780938000000 | 2.945506000000 |
| C | 0.000000000000 | -3.458456000000 | 6.694903000000 |
| C | 0.000000000000 | -2.492984000000 | 7.656326000000 |
| C | 0.000000000000 | 2.492984000000 | 7.656326000000 |
| C | 0.000000000000 | 3.458456000000 | 6.694903000000 |
| C | 0.000000000000 | 3.459665000000 | 1.679951000000 |
| C | 0.000000000000 | 2.494818000000 | 0.719321000000 |
| C | 0.000000000000 | -3.459665000000 | 1.679951000000 |
| C | 0.000000000000 | -2.494818000000 | 0.719321000000 |
| H | 0.000000000000 | -4.529625000000 | 6.825027000000 |
| H | 0.000000000000 | 4.529625000000 | 6.825027000000 |
| H | 0.000000000000 | 4.530811000000 | 1.549679000000 |
| H | 0.000000000000 | -4.530811000000 | 1.549679000000 |
| H | 0.000000000000 | 4.483602000000 | 4.187077000000 |
| H | 0.000000000000 | -4.483602000000 | 4.187077000000 |
| Zn | 0.000000000000 | 0.000000000000 | -4.186783000000 |
| C | 0.000000000000 | 0.000000000000 | -0.737158000000 |
| C | 0.000000000000 | 3.400567000000 | -4.186717000000 |
| C | 0.000000000000 | 0.000000000000 | -7.639528000000 |
| C | 0.000000000000 | -3.400567000000 | -4.186717000000 |
| N | 0.000000000000 | 1.430766000000 | -5.629787000000 |
| N | 0.000000000000 | 1.430498000000 | -2.745983000000 |
| N | 0.000000000000 | -1.430498000000 | -2.745983000000 |
| N | 0.000000000000 | -1.430766000000 | -5.629787000000 |
| C | 0.000000000000 | -2.780938000000 | -2.945506000000 |
| C | 0.000000000000 | -1.230973000000 | -1.407112000000 |
| C | 0.000000000000 | 1.230973000000 | -1.407112000000 |
| C | 0.000000000000 | 2.780938000000 | -2.945506000000 |
| C | 0.000000000000 | -2.779597000000 | -5.431213000000 |
| C | 0.000000000000 | -1.230637000000 | -6.969873000000 |
| C | 0.000000000000 | 1.230637000000 | -6.969873000000 |
| C | 0.000000000000 | 2.779597000000 | -5.431213000000 |
| C | 0.000000000000 | -3.459665000000 | -1.679951000000 |
| C | 0.000000000000 | -2.494818000000 | -0.719321000000 |
| C | 0.000000000000 | 2.494818000000 | -0.719321000000 |
| C | 0.000000000000 | 3.459665000000 | -1.679951000000 |
| C | 0.000000000000 | 3.458456000000 | -6.694903000000 |
| C | 0.000000000000 | 2.492984000000 | -7.656326000000 |
| C | 0.000000000000 | -3.458456000000 | -6.694903000000 |
| C | 0.000000000000 | -2.492984000000 | -7.656326000000 |
| H | 0.000000000000 | -4.530811000000 | -1.549679000000 |

| | | | |
|---|---|---|---|
| C | 0.000000000000 | -3.468610000000 | 10.049008000000 |
| C | 0.000000000000 | -2.500906000000 | 9.082402000000 |
| H | 0.000000000000 | -4.539665000000 | 15.186103000000 |
| H | 0.000000000000 | -2.644037000000 | 17.090222000000 |
| H | 0.000000000000 | 2.644037000000 | 17.090222000000 |
| H | 0.000000000000 | 4.539665000000 | 15.186103000000 |
| H | 0.000000000000 | 4.539778000000 | 9.920004000000 |
| H | 0.000000000000 | -4.539778000000 | 9.920004000000 |
| H | 0.000000000000 | 0.000000000000 | 17.050471000000 |
| H | 0.000000000000 | 4.489471000000 | 12.547735000000 |
| H | 0.000000000000 | -4.489471000000 | 12.547735000000 |
| Zn | 0.000000000000 | 0.000000000000 | 4.174582000000 |
| C | 0.000000000000 | 0.000000000000 | 7.651444000000 |
| C | 0.000000000000 | 3.402034000000 | 4.183059000000 |
| C | 0.000000000000 | 0.000000000000 | 0.700789000000 |
| C | 0.000000000000 | -3.402034000000 | 4.183059000000 |
| N | 0.000000000000 | 1.434917000000 | 2.726321000000 |
| N | 0.000000000000 | 1.432427000000 | 5.632416000000 |
| N | 0.000000000000 | -1.432427000000 | 5.632416000000 |
| N | 0.000000000000 | -1.434917000000 | 2.726321000000 |
| C | 0.000000000000 | -2.791896000000 | 5.430093000000 |
| C | 0.000000000000 | -1.246782000000 | 6.964290000000 |
| C | 0.000000000000 | 1.246782000000 | 6.964290000000 |
| C | 0.000000000000 | 2.791896000000 | 5.430093000000 |
| C | 0.000000000000 | -2.798369000000 | 2.932853000000 |
| C | 0.000000000000 | -1.256084000000 | 1.397165000000 |
| C | 0.000000000000 | 1.256084000000 | 1.397165000000 |
| C | 0.000000000000 | 2.798369000000 | 2.932853000000 |
| C | 0.000000000000 | -3.470588000000 | 6.679090000000 |
| C | 0.000000000000 | -2.500839000000 | 7.649543000000 |
| C | 0.000000000000 | 2.500839000000 | 7.649543000000 |
| C | 0.000000000000 | 3.470588000000 | 6.679090000000 |
| C | 0.000000000000 | 3.478819000000 | 1.690743000000 |
| C | 0.000000000000 | 2.508090000000 | 0.714381000000 |
| C | 0.000000000000 | -3.478819000000 | 1.690743000000 |
| C | 0.000000000000 | -2.508090000000 | 0.714381000000 |
| H | 0.000000000000 | -4.541918000000 | 6.807650000000 |
| H | 0.000000000000 | 4.541918000000 | 6.807650000000 |
| H | 0.000000000000 | 4.550238000000 | 1.563887000000 |
| H | 0.000000000000 | -4.550238000000 | 1.563887000000 |
| H | 0.000000000000 | 4.486227000000 | 4.185642000000 |
| H | 0.000000000000 | -4.486227000000 | 4.185642000000 |
| Zn | 0.000000000000 | 0.000000000000 | -4.174582000000 |
| C | 0.000000000000 | 0.000000000000 | -0.700789000000 |
| C | 0.000000000000 | 3.402034000000 | -4.183059000000 |
| C | 0.000000000000 | 0.000000000000 | -7.651444000000 |
| C | 0.000000000000 | -3.402034000000 | -4.183059000000 |
| N | 0.000000000000 | 1.432427000000 | -5.632416000000 |
| N | 0.000000000000 | 1.434917000000 | -2.726321000000 |
| N | 0.000000000000 | -1.434917000000 | -2.726321000000 |
| N | 0.000000000000 | -1.432427000000 | -5.632416000000 |
| C | 0.000000000000 | -2.798369000000 | -2.932853000000 |
| C | 0.000000000000 | -1.256084000000 | -1.397165000000 |
| C | 0.000000000000 | 1.256084000000 | -1.397165000000 |
| C | 0.000000000000 | 2.798369000000 | -2.932853000000 |
| C | 0.000000000000 | -2.791896000000 | -5.430093000000 |
| C | 0.000000000000 | -1.246782000000 | -6.964290000000 |
| C | 0.000000000000 | 1.246782000000 | -6.964290000000 |
| C | 0.000000000000 | 2.791896000000 | -5.430093000000 |
| C | 0.000000000000 | -3.478819000000 | -1.690743000000 |
| C | 0.000000000000 | -2.508090000000 | -0.714381000000 |
| C | 0.000000000000 | 2.508090000000 | -0.714381000000 |
| C | 0.000000000000 | 3.478819000000 | -1.690743000000 |
| C | 0.000000000000 | 3.470588000000 | -6.679090000000 |
| C | 0.000000000000 | 2.500839000000 | -7.649543000000 |
| C | 0.000000000000 | -3.470588000000 | -6.679090000000 |
| C | 0.000000000000 | -2.500839000000 | -7.649543000000 |
| H | 0.000000000000 | -4.550238000000 | -1.563887000000 |

| | | | |
|---|---|---|---|
| H | 0.000000000000 | 4.530811000000 | -1.549679000000 |
| H | 0.000000000000 | 4.529625000000 | -6.825027000000 |
| H | 0.000000000000 | -4.529625000000 | -6.825027000000 |
| H | 0.000000000000 | 4.483602000000 | -4.187077000000 |
| H | 0.000000000000 | -4.483602000000 | -4.187077000000 |
| Zn | 0.000000000000 | 0.000000000000 | -12.569707000000 |
| C | 0.000000000000 | 0.000000000000 | -15.977162000000 |
| C | 0.000000000000 | -3.405425000000 | -12.556352000000 |
| C | 0.000000000000 | 0.000000000000 | -9.116103000000 |
| C | 0.000000000000 | 3.405425000000 | -12.556352000000 |
| N | 0.000000000000 | -1.429812000000 | -11.124319000000 |
| N | 0.000000000000 | -1.443528000000 | -14.009272000000 |
| N | 0.000000000000 | 1.443528000000 | -14.009272000000 |
| N | 0.000000000000 | 1.429812000000 | -11.124319000000 |
| C | 0.000000000000 | 2.785446000000 | -13.805047000000 |
| C | 0.000000000000 | 1.241904000000 | -15.356481000000 |
| C | 0.000000000000 | -1.241904000000 | -15.356481000000 |
| C | 0.000000000000 | -2.785446000000 | -13.805047000000 |
| C | 0.000000000000 | 2.782198000000 | -11.321964000000 |
| C | 0.000000000000 | 1.229281000000 | -9.786305000000 |
| C | 0.000000000000 | -1.229281000000 | -9.786305000000 |
| C | 0.000000000000 | -2.782198000000 | -11.321964000000 |
| C | 0.000000000000 | 3.466414000000 | -15.070106000000 |
| C | 0.000000000000 | 2.510520000000 | -16.030828000000 |
| C | 0.000000000000 | -2.510520000000 | -16.030828000000 |
| C | 0.000000000000 | -3.466414000000 | -15.070106000000 |
| C | 0.000000000000 | -3.459088000000 | -10.052357000000 |
| C | 0.000000000000 | -2.494380000000 | -9.095065000000 |
| C | 0.000000000000 | 3.459088000000 | -10.052357000000 |
| C | 0.000000000000 | 2.494380000000 | -9.095065000000 |
| H | 0.000000000000 | 4.537881000000 | -15.197414000000 |
| H | 0.000000000000 | 2.643308000000 | -17.101647000000 |
| H | 0.000000000000 | -2.643308000000 | -17.101647000000 |
| H | 0.000000000000 | -4.537881000000 | -15.197414000000 |
| H | 0.000000000000 | -4.530099000000 | -9.920765000000 |
| H | 0.000000000000 | 4.530099000000 | -9.920765000000 |
| H | 0.000000000000 | 0.000000000000 | -17.060277000000 |
| H | 0.000000000000 | -4.488377000000 | -12.554108000000 |
| H | 0.000000000000 | 4.488377000000 | -12.554108000000 |

| | | | |
|---|---|---|---|
| H | 0.000000000000 | 4.550238000000 | -1.563887000000 |
| H | 0.000000000000 | 4.541918000000 | -6.807650000000 |
| H | 0.000000000000 | -4.541918000000 | -6.807650000000 |
| H | 0.000000000000 | 4.486227000000 | -4.185642000000 |
| H | 0.000000000000 | -4.486227000000 | -4.185642000000 |
| Zn | 0.000000000000 | 0.000000000000 | -12.550425000000 |
| C | 0.000000000000 | 0.000000000000 | -15.967595000000 |
| C | 0.000000000000 | -3.406246000000 | -12.547681000000 |
| C | 0.000000000000 | 0.000000000000 | -9.085790000000 |
| C | 0.000000000000 | 3.406246000000 | -12.547681000000 |
| N | 0.000000000000 | -1.432884000000 | -11.104713000000 |
| N | 0.000000000000 | -1.443141000000 | -13.998547000000 |
| N | 0.000000000000 | 1.443141000000 | -13.998547000000 |
| N | 0.000000000000 | 1.432884000000 | -11.104713000000 |
| C | 0.000000000000 | 2.787874000000 | -13.793814000000 |
| C | 0.000000000000 | 1.244179000000 | -15.343859000000 |
| C | 0.000000000000 | -1.244179000000 | -15.343859000000 |
| C | 0.000000000000 | -2.787874000000 | -13.793814000000 |
| C | 0.000000000000 | 2.789461000000 | -11.306099000000 |
| C | 0.000000000000 | 1.242540000000 | -9.768736000000 |
| C | 0.000000000000 | -1.242540000000 | -9.768736000000 |
| C | 0.000000000000 | -2.789461000000 | -11.306099000000 |
| C | 0.000000000000 | 3.468208000000 | -15.058660000000 |
| C | 0.000000000000 | 2.511999000000 | -16.019417000000 |
| C | 0.000000000000 | -2.511999000000 | -16.019417000000 |
| C | 0.000000000000 | -3.468208000000 | -15.058660000000 |
| C | 0.000000000000 | -3.468610000000 | -10.049008000000 |
| C | 0.000000000000 | -2.500906000000 | -9.082402000000 |
| C | 0.000000000000 | 3.468610000000 | -10.049008000000 |
| C | 0.000000000000 | 2.500906000000 | -9.082402000000 |
| H | 0.000000000000 | 4.539665000000 | -15.186103000000 |
| H | 0.000000000000 | 2.644037000000 | -17.090222000000 |
| H | 0.000000000000 | -2.644037000000 | -17.090222000000 |
| H | 0.000000000000 | -4.539665000000 | -15.186103000000 |
| H | 0.000000000000 | -4.539778000000 | -9.920004000000 |
| H | 0.000000000000 | 4.539778000000 | -9.920004000000 |
| H | 0.000000000000 | 0.000000000000 | -17.050471000000 |
| H | 0.000000000000 | -4.489471000000 | -12.547735000000 |
| H | 0.000000000000 | 4.489471000000 | -12.547735000000 |

## References

1. Gaussian 16, Revision C.01, M. J. Frisch, G. W. Trucks, H. B. Schlegel, G. E. Scuseria, M. A. Robb, J. R. Cheeseman, G. Scalmani, V. Barone, G. A. Petersson, H. Nakatsuji, X. Li, M. Caricato, A. V. Marenich, J. Bloino, B. G. Janesko, R. Gomperts, B. Mennucci, H. P. Hratchian, J. V. Ortiz, A. F. Izmaylov, J. L. Sonnenberg, D. Williams-Young, F. Ding, F. Lipparini, F. Egidi, J. Goings, B. Peng, A. Petrone, T. Henderson, D. Ranasinghe, V. G. Zakrzewski, J. Gao, N. Rega, G. Zheng, W. Liang, M. Hada, M. Ehara, K. Toyota, R. Fukuda, J. Hasegawa, M. Ishida, T. Nakajima, Y. Honda, O. Kitao, H. Nakai, T. Vreven, K. Throssell, J. A. Montgomery, Jr., J. E. Peralta, F. Ogliaro, M. J. Bearpark, J. J. Heyd, E. N. Brothers, K. N. Kudin, V. N. Staroverov, T. A. Keith, R. Kobayashi, J. Normand, K. Raghavachari, A. P. Rendell, J. C. Burant, S. S. Iyengar, J. Tomasi, M. Cossi, J. M. Millam, M. Klene, C. Adamo, R. Cammi, J. W. Ochterski, R. L. Martin, K. Morokuma, O. Farkas, J. B. Foresman, and D. J. Fox, Gaussian, Inc., Wallingford CT, 2016.
2. J.-D. Chai and M. Head-Gordon, *J. Chem. Phys.*, 2008, **128**, 084106
3. F. Weigend and R. Ahlrichs, *Phys. Chem. Chem. Phys.*, 2005, **7**, 3297-3305.
4. D. W. Szczepanik, M. Solà, M. Andrzejak, B. Pawełek, J. Dominikowska, M. Kukułka, K. Dyduch, T. M. Krygowski and H. Szatylowicz, *J. Comput. Chem.*, 2017, **38**, 1640-1654.
5. C. Riplinger and F. Neese, *J. Chem. Phys.* , 2013, **138**, 034106.
6. C. Riplinger, B. Sandhoefer, A. Hansen and F. Neese, *J. Chem. Phys.*, 2013, **139**, 134101.
7. C. Riplinger, P. Pinski, U. Becker, E. F. Valeev and F. Neese, *J. Chem. Phys.*, 2016, **144**, 024109.
8. F. Neese, *WIREs Comput. Mol. Sci.*, 2022, **12**, e1606.
9. T. J. Lee and P. R. Taylor, *Int. J. Quantum Chem.*, 1989, **36**, 199-207.
10. G. Monaco, F. F. Summa and R. Zanasi, *J. Chem. Inf. Model.*, 2021, **61**, 270-283.
11. P. Lazzeretti, M. Malagoli and R. Zanasi, *Chem. Phys. Lett.*, 1994, **220**, 299-304.
12. J. R. Cheeseman, G. W. Trucks, T. A. Keith and M. J. Frisch, *J. Chem. Phys.*, 1996, **104**, 5497-5509.
13. S. Klod and E. Kleinpeter, *J. Chem. Soc., Perkin Trans.,* 2001, **2**, 1893-1898.
14. Z. Liu, T. Lu and Q. Chen, *Carbon*, 2020, **165**, 468-475.
15. T. Lu and F. Chen, *J. Comput. Chem.*, 2012, **33**, 580-592.
16. D. W. Szczepanik, M. Andrzejak, K. Dyduch, E. Żak, M. Makowski, G. Mazur and J. Mrozek, *Phys. Chem. Chem. Phys.*, 2014, **16**, 20514-20523.
17. D. W. Szczepanik, M. Andrzejak, J. Dominikowska, B. Pawełek, T. M. Krygowski, H. Szatylowicz and M. Solà, *Phys. Chem. Chem. Phys.*, 2017, **19**, 28970-28981.
18. T. M. Krygowski, H. Szatylowicz, O. A. Stasyuk, J. Dominikowska, M. Palusiak, *Chem. Rev.*, **2014**, *114*, 6383-6422.
19. F. Feixas, E. Matito, J. Poater, M. Solà, *Chem. Soc. Rev.*, **2015**, *44*, 6434-6451.
20. P. Bultinck, R. Ponec, S. Van Damme, *J. Phys. Org. Chem.*, **2005**, *18*, 706-718.
21. E. Matito, *Phys. Chem. Chem. Phys.* **2016**, *18*, 11839-11846.
22. C. García-Fernández, E. Sierda, M. Abadía, B. Bugenhagen, M. H. Prosenc, R. Wiesendanger, M. Bazarnik, J. E. Ortega, J. Brede, E. Matito et al., *J. Phys. Chem. C* **2017**, *121*, 27118-27125.
23. E. Matito, M. Duran, M. Solà, *J. Chem. Phys.* **2004**, *122*, 014109.
24. R. F. W. Bader, *Journal*, 1990, DOI: 10.1093/oso/9780198551683.001.0001.
25. R. F. W. Bader, *Chem. Rev.*, 1991, **91**, 893-928.
26. T. A. Keith, *Journal*, 2019.
27. T. A. Keith, *Chem. Phys.*, 1996, **213**, 123-132.
28. T. A. Keith and R. F. W. Bader, *Chem. Phys. Lett.*, 1993, **210**, 223-231.
29. T. A. Keith and R. F. W. Bader, *Chem. Phys. Lett.*, 1992, **194**, 1-8.
30. Matito, E. *ESI-3D: Electron Sharing Indices Program for 3D Molecular Space Partitioning*; Institute of Computational Chemistry and Catalysis, University of Girona, 2006.